

US

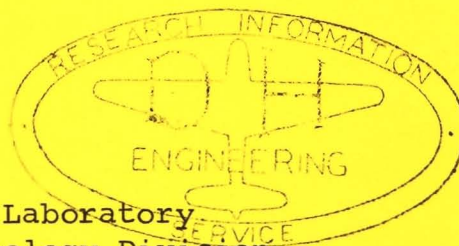
AIR FORCE ML 64-401

AF ML TR-64-401

The Structural Reliability of Airframes

TECHNICAL REPORT NO. AFML-TR-64-401

December 1964



AF Materials Laboratory
Research and Technology Division
Air Force Systems Command
Wright-Patterson Air Force Base, Ohio

Project No. 2(8-7351), Task No. 735106

(Prepared under Contract No. AF 33(616)-7042
by Columbia University, New York, New York;
A. M. Freudenthal and A. O. Payne, authors)

NOTICES

When Government drawings, specifications, or other data are used for any purpose other than in connection with a definitely related Government procurement operation, the United States Government thereby incurs no responsibility nor any obligation whatsoever; and the fact that the Government may have formulated, furnished, or in any way supplied the said drawings, specifications, or other data, is not to be regarded by implication or otherwise as in any manner licensing the holder or any other person or corporation, or conveying any rights or permission to manufacture, use, or sell any patented invention that may in any way be related thereto.

Qualified requesters may obtain copies of this report from the Defense Documentation Center (DDC), (formerly ASTIA), Cameron Station, Bldg. 5, 5010 Duke Street, Alexandria, Virginia, 22314.

This report has been released to the Office of Technical Services, U.S. Department of Commerce, Washington 25, D. C., for sale to the general public.

Copies of this report should not be returned to the Research and Technology Division, Wright-Patterson Air Force Base, Ohio, unless return is required by security considerations, contractual obligations, or notice on a specific document.

The Structural Reliability of Airframes

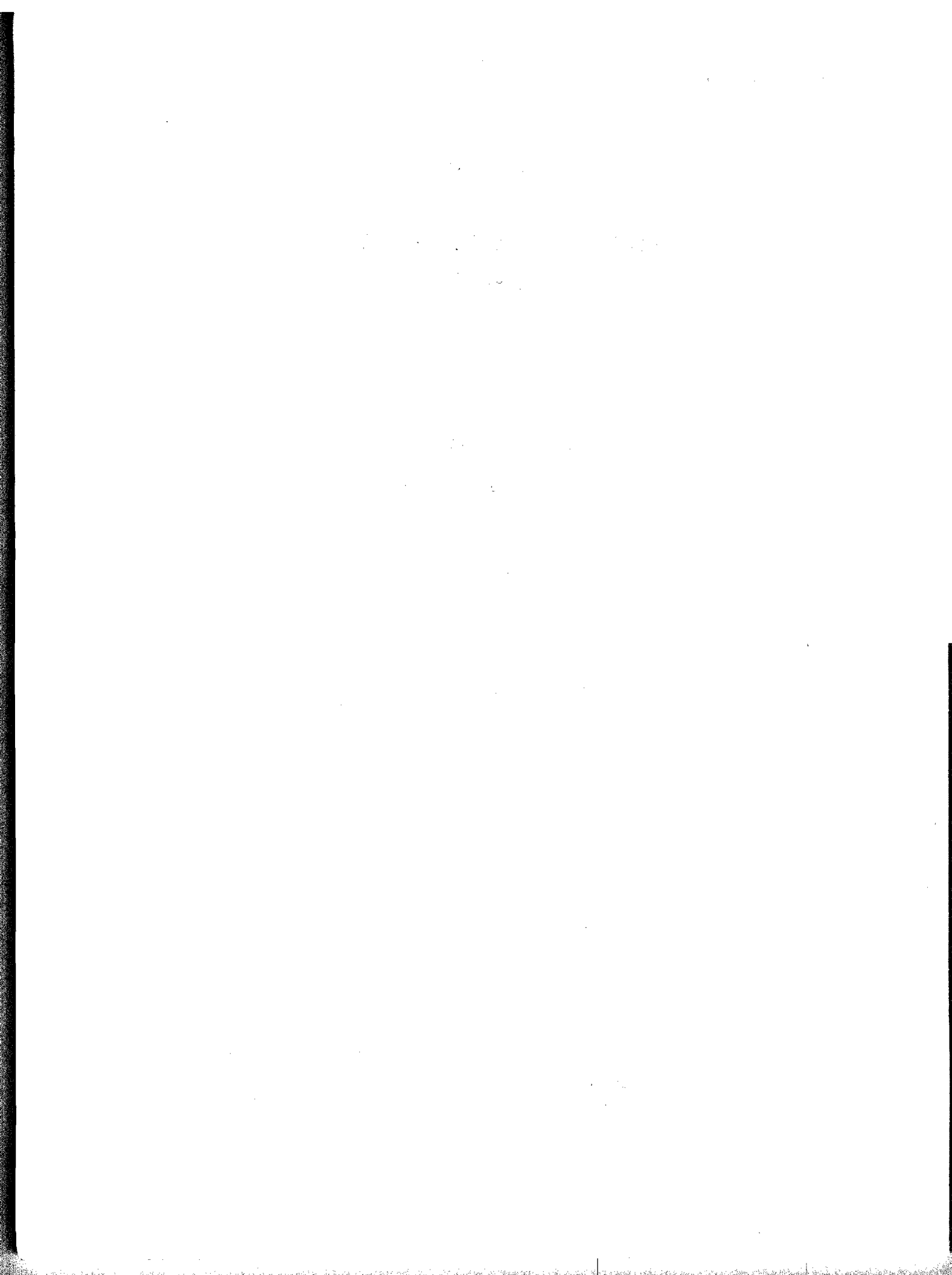
TECHNICAL REPORT NO. AFML-TR-64-401

December 1964

AF Materials Laboratory
Research and Technology Division
Air Force Systems Command
Wright-Patterson Air Force Base, Ohio

Project No. 2(8-7351), Task No. 735106

(Prepared under Contract No. AF 33(616)-7042
by Columbia University, New York, New York;
A. M. Freudenthal and A. O. Payne, authors)

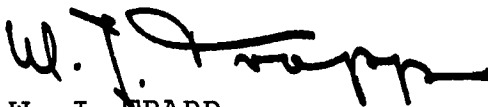


ABSTRACT

The theory of reliability estimation developed in previous reports (WADD TR61-53, ML-TDR-64-300) has been applied to three types of aircraft, a civilian transport, a heavy bomber and a fighter designed by current procedures, for which operational records, multiple structural tests and records of service experience are available. Failure rates for critical ultimate load conditions have been evaluated on the basis of data obtained from various sources and compared with service experience. Lives associated with equal risk of ultimate load failure and fatigue failure (or initial structural fatigue damage) have also been computed.

The obtained numerical values which reflect current design practices can serve as the basis for a rational comparative reliability analysis of new designs involving new materials and different design criteria and missions spectra and profiles.

This technical documentary report has been reviewed and is approved.



W. J. TRAPP
Chief, Strength and Dynamics Branch
Metals and Ceramics Division
AF Materials Laboratory

TABLE OF CONTENTS

	PAGE
SUMMARY	1
1. INTRODUCTION	4
2. FLIGHT LOADS	6
3. DISTRIBUTION OF STATIC STRENGTH	10
4. ULTIMATE STRENGTH ANALYSIS	20
5. FATIGUE STRENGTH ANALYSIS	35
6. DISCUSSION OF RESULTS	42
7. CONCLUSIONS	49
REFERENCES	51

TABLES

TABLE		PAGE
1.	Service Load Data: (a) Atmospheric Gusts, (b) Maneuver Accelerations	53
2.	Variation in Amount of Turbulence with Altitude .	55
3.	Data on Ultimate Strength of Structures	56
4.	Reliability Calculations: (a) Gust Loads, (b) Maneuver Loads	57
5.	Comparison of Failure Rates: (a) Ultimate Failure, (b) Fatigue Failure	62
6.	Fatigue Lives: Initial Failure of Heavy Bomber	64
7.	Estimation of Fatigue Sensitivity Factors: (a) Fatigue Sensitivity Factor at Seven Life Times (b) Life Time for Equal Failure Risks	65

ILLUSTRATIONS

FIGURE	PAGE
1. Probability Distribution for Thunderstorm Gusts .	67
2. Probability Distribution for Gusts: General Operation	68
3. Total Gust Counts per Mile: General Operation .	69
4. Probability Distribution for Lateral Gusts . . .	70
5. Frequency Distributions for Maneuver Accelera- tions: Fighter Aircraft.	71
6. Vertical Acceleration Data for Heavy Bomber . . .	72
7. Probability Distribution for Structural Resist- ance	73
8. Integration of Reliability Function in Terms of R and S	74
9. Probability of Failure in Thunderstorm Gusts . .	75
10. Probability of Failure under a Thunderstorm Gust for Various Safety Factors: Upgust, $p = 0.1$. .	76
11. Probability of Failure under a Thunderstorm Gust for Various Safety Factors: Upgust, $p = 0.5$. .	77
12. Probability of Failure under a Thunderstorm Gust for Various Safety Factors: Downgust, $p = 0.1$.	78
13. Probability of Failure under a Thunderstorm Gust for Various Safety Factors: Downgust, $p = 0.5$.	79
14. Probability of Failure under a Thunderstorm Gust as a Function of K_n	80
15. Probabilities of Failure as a Function of v . . .	81
16. Probability of Failure as a Function of Struc- tural Resistance R and Service Load S	82

FIGURE		PAGE
17.	Probability of Failure of Lighter Aircraft in Various Missions	83
18.	Comparison of Failure Rates under Various Load Spectra	84
19.	Probability Distribution of Fatigue Life for Heavy Bomber	85
20.	Non-Dimensional Risk Function (Log-Normal Distribution)	86

SUMMARY

The theory developed previously for determining the probability of structural failure under both ultimate and fatigue loading¹ has been applied to certain aircraft structures for which operational records and multiple structural tests are available and the results of the analysis have been compared with results from service experience. An analysis has also been made of the effect of various design and specification parameters on the probability of failure under ultimate load.

The method used takes account of the statistical variation of operational loads acting on the aircraft as well as of the ultimate strength and fatigue life of the structure and has been applied to the following representative cases: (a) civil transport aircraft, (b) heavy bomber aircraft, and (c) fighter aircraft. In each case the "risk" of ultimate load failure (r_u), the risk of fatigue failure (r_F) and the fatigue sensitivity factor¹ [$f(N) = \frac{r_F}{r_u}$] have been determined.

For ultimate load failure reasonable agreement with service experience has been found and the maximum values of

Manuscript released by the authors December 1964 for publication as an RTD Technical Documentary Report.

the computed failure rates associated with current design procedures are as follows:

- (a) Civil transport: 10^{-7} per hour (thunderstorm downgust critical)
- (b) Heavy bomber: 10^{-8} per hour (lateral gust on tail assembly critical)
- (c) Fighter: 10^{-5} per hour (upward maneuver load critical)

The actual failure rates may vary by several orders of magnitude depending on the assumed design and operating conditions and the proposed method of reliability analysis makes it possible to evaluate the effect of a change in such conditions on failure rate. Comparison with service experience indicates that the theory provides an adequate method of reliability prediction.

The risk of fatigue failure is a function of the life (N); introducing the life N_0 at which the risks of ultimate load and fatigue failure are equal as a design criterion these lives N_0 at which for current design procedures the structures become fatigue critical are:

- (a) Civil transport (design service life for ultimate load assumed to be 20,000 hours)

$$N_0 = 15,000 \text{ hours}$$

- (b) Heavy bomber for mission profiles including low level flight (initial fatigue failure)

$$N_0 = 960 \text{ hours}$$

- (c) Fighter

$$N_0 = 1,900 \text{ hours}$$

The associated reliability figures for ultimate load design are of the order of $R = 0.99$ for (a) and (b) and $R = 0.94$ for (c). The above figures indicate that for currently assumed operational lives and considered operational load spectra the risk of fatigue failure is critical in all cases considered in this analysis.

Having established the numerical values for ultimate load failure rates and for fatigue lives at equal risk of ultimate load and fatigue failure reflecting current design practices, a rational comparative reliability analysis of new designs becomes possible using different design criteria, different structural materials and different mission spectra and profiles, but retaining the method of analysis outlined and illustrated in this report.

1. INTRODUCTION

The rising importance, in recent years, of the problem of structural reliability is largely a result of the increasing size and complexity of aircraft structures as well as the rapid growth of aircraft operations.

To insure adequate safety of civil transport aircraft, it is necessary that the probability of structural failure be negligible compared to the normal hazards involved, as in any form of transport. In the case of military aircraft the risk of structural collapse should be much lower than the accepted operational risk. To meet these requirements the probability of structural failure at any stage must be determined. While this problem has attracted the attention of a number of authorities,^{2,3,4} a solution of the general case in terms of known parameters has not yet evolved.

An approach to the problem has recently been made based on reliability theory,¹ and the purpose of the present investigation is as follows:

(a) to investigate the probability of fatigue and ultimate load failure when the various design and operational parameters are varied;

(b) to use data obtained from service operations and to compare the performance predicted with that actually achieved for both civil and military aircraft types.

These objectives have required the assembling of comprehensive data on the ultimate strength and fatigue strength of various structures, as well as flight load data from a variety of aircraft operations and service data from civil and military aircraft including records of structural failures.

The program has been supported by the Research and Technical Division of the United States Air Force Systems Command; the continuous interest and active assistance in all phases of this program of Mr. W. J. Trapp, Chief, Strength and Dynamics Branch, Air Force Materials Laboratory, is gratefully acknowledged. The program has received cooperation from the Aeronautical Research Laboratories in Australia; the Research Institute, University of Dayton; the United States Naval Air Engineering Center; the National Aeronautics and Space Administration; the Federal Aviation Agency; leading aircraft manufacturing firms in the United States; the Royal Aircraft Establishment in the United Kingdom; and Sud-Aviation Aircraft Company in France.

2. FLIGHT LOADS

Flight load data have been obtained from various sources and have been presented here in two broad divisions: atmospheric gusts and aircraft maneuvers. All data available were in the form of frequency distributions which, for our purposes, have been transformed into probability distributions associated with a value for the total number of load occurrences per hour (or per mile). Equations for the probability distributions and the total frequencies of occurrence appear in Table 1.

(a) Atmospheric Gusts

These data refer primarily to the effect of atmospheric turbulence; the effect of any maneuver loads that occur is included since these effects are minor where gust loads are relevant.

(i) Thunderstorm Gust Data

Results from the National Advisory Committee for Aeronautics investigations in 1941-42, 1946 and 1947 on gust frequencies in thunderstorms have been obtained from Tolefson.⁵ A regression analysis has been carried out and the various results have been combined to give the probability spectrum presented in Fig. 1 associated with an estimated

14 gusts per mile. The average percentage (α %) of the total distance spent in thunderstorms has been estimated as a function of operating height;⁶ these data have been reproduced in Table 2. For an average cruising speed V_C the average number of loads per hour is therefore $14 \times 2 \times 10^{-2} \times V_C = 0.14\alpha V_C$.

(ii) General Data for Civil Transports

Comprehensive gust load data have been obtained by the Royal Aircraft Establishment from civil transports operating over world-wide routes.⁷ These data are reproduced as a probability distribution in Fig. 2. The total number of gusts per nautical mile is shown as a function of height in Fig. 3.

(iii) Lateral Gust Data

The only available data on lateral gust frequencies are those recently obtained by the University of Dayton on United States heavy bombers.⁸ Data for both high- and low-level operations have been presented as probability distributions in Fig. 4 with the associated gust counts per hour.

(b) Maneuver Accelerations

(i) Fighter Aircraft

Maneuver load data on fighter aircraft from a variety of sources are reproduced in Fig. 5. The United

States and British data are the average of a large number of records on different fighter aircraft types. The United States data are based on fighters in the Air Force FII category with an ultimate load factor $n_u = 11$.

Variation occurs according to role, the ground-attack mission giving more frequent positive (upward) acceleration counts than any other mission. However, the distribution with the density

$$p(\Delta_n)d\Delta_n = \frac{2}{\sqrt{2\pi}} \sigma_n e^{-\frac{\Delta_n^2}{2\sigma_n^2}} d\Delta_n \quad \Delta_n > 0 \quad (2.1)$$

has been found to give a consistently good representation for the positive accelerations Δ_n except at very small acceleration values. Eq. (2.1) represents the density function of a normal distribution with mean zero truncated at the mean for positive values with normalizing factor 2. All missions can therefore be represented by taking suitable values for the mission parameter σ_n as shown in Table I.

This procedure is quite satisfactory for the prediction of ultimate load failure. For general application in fatigue calculations, however, it is recommended that an exponential distribution be added for both positive and negative loads associated with their total occurrences per hour to give a frequency spectrum of fatigue loads.

(ii) Bomber Aircraft

Combined gust and maneuver load data on United States heavy bombers are presented as a probability distribution of accelerations in Fig. 6. Unlike the preceding data, which are of general application, these results refer to the particular type only. In order to facilitate their application in the calculations in Section 3, these data are presented in a form which includes the effect of the fleet operating characteristics.

3. DISTRIBUTION OF STATIC STRENGTH

To investigate the variability of ultimate strength of aircraft structures, multiple-test data from 11 different types of structure and 9 types of mainplane panels were assembled for analysis as shown in Table 3. The panels were all loaded to failure in compression but the different types of structures were tested under various loading cases and tension, compression and shear failures are represented in these results. The data from these 19 groups therefore give a good representation of the ultimate strength behavior of aircraft structures in general.

(a) Analysis of Data

Analysis of the data suggests that a single distribution of the ultimate failing load about the mean value can be obtained, irrespective of the type of structure tested or its mode of failure.

To test this hypothesis against the experimental data, the population means μ_{R_i} have to be estimated in each group by the experimental mean \bar{R}_i which for some groups is determined on only 3 or 4 specimens. In an attempt to reduce this bias, the

variate $\xi = \frac{x}{\sigma_x}$ has been represented by the standardized variate

$$\frac{R_i - \bar{R}_i}{\sigma(R_i - \bar{R}_i)} = \frac{R_i - \bar{R}_i}{\sigma_R \sqrt{\frac{r_i - 1}{r_i}}}$$

which has been estimated by

$$Y_m = \frac{R_i - \bar{R}_i}{\bar{R}_i S_x} \sqrt{\frac{r_i}{r_i - 1}}$$

The values $R_i S_x$ for estimating σ_R are based on the sample means \bar{R}_i and the combined standard deviation S_x determined on the total of 170 values.

The $\overset{\text{(values)}}{Y_m}$ have been calculated for every specimen in each group and then arranged in ascending order of magnitude ($m = 1, 2, \dots, n$). These values have been plotted against the mean relative frequency $\frac{m}{n+1}$ in Fig. 7; it is found that the $n = 170$ points so obtained are all distributed along a smooth curve with no tendency to segregate according to groups. To show this the 10 most extreme points in both tails of the distribution have been identified by their group letter (as listed in Table 3) and the extreme points for each group are also identified in the array of 170 points by their group letter.

The probability distribution as represented by the data points is symmetric; it follows the normal distribution closely near the mean but diverges from it considerably in the vicinity of the extreme values.

Of the many distributions tried, the "t" distribution was the only one giving a satisfactory representation; the excellent fit shown in Fig. 7 was obtained using the "t" distribution with 3 degrees of freedom and setting $Y = \frac{3}{4} t$.

Hence

$$P_Y(Y) = P_Y \left(\frac{R_i - \bar{R}_i}{R_i S_X} \sqrt{\frac{r_i}{r_i - 1}} \right) = P_{(v_t=3)} \left(\frac{4}{3} Y \right) \quad (3.1)$$

where $P_{v_t=3}(t)$ is the probability function of the "t" distribution with 3 degrees of freedom.

It then follows that the variate $\frac{x}{S_X} = \frac{R_i - \mu_{R_i}}{\mu_{R_i} S_X}$ based

on the true means μ_{R_i} has the distribution

$$P \left(\frac{x}{S_X} \right) = P_{v_t=3} \left(\frac{4}{3} \cdot \frac{x}{S_X} \right) \quad (3.2)$$

while the true standardized variable $\xi = \frac{R - \mu_R}{\mu_R \sigma_X}$ must have the distribution

$$P(\xi) = P(\sqrt{3} \xi) = P_{\nu_t=3} \left(\sqrt{3} \frac{x}{\sigma_X} \right) \quad (3.3)$$

since $P_{\nu_t=3}(t)$ has variance of 3.

Equivalence of (3.3) and (3.2) gives $\sigma_x = \frac{3\sqrt{3}}{4} S_X = 1.299 S_X$ for best fit of the "t" distribution shown in Fig. 7.

A comparison of both S_X^2 and σ_X^2 with the sample variances of the various groups of data has been carried out using the F test. The results presented in Table 3 show that both S_X^2 and σ_X^2 as population variances give no significant difference from the sample variances in 10 cases out of the 19. However, since the F test refers to the normal distribution it will prove a too severe test for the compatibility of variances in a "t" distribution of three degrees of freedom. The 9 cases in which there is a significant difference do not therefore necessarily reject the hypothesis of a common "t" distribution. But the results do indicate that a comparison with the sample variances does not reject the value of σ_X^2 as the population variance in favor of the value of S_X^2 .

The value σ_X^2 is therefore taken for the variance of $x = \frac{R-\mu_R}{\mu_R}$. Hence

$$p_X(x) = p(\xi) \frac{d\xi}{dx} = \frac{2}{\pi} \left(1 + \frac{x^2}{\sigma_X^2}\right)^{-2} \cdot \frac{1}{\sigma_X} = \frac{2\sigma_X^3}{\pi(\sigma_X^2 + x^2)^2} \quad (3.4)$$

$$P_X(X) = \int_{-\infty}^X p(x) dx = \frac{\sigma_X^3 x}{\pi(\sigma_X^2 + x^2)} + \frac{1}{\pi} \arctan \frac{x}{\sigma_X} + \frac{1}{2} \quad (3.5)$$

Within the region covered by the data ($-.15 \leq x \leq .15$) it has therefore been possible to establish for the variation in relative strength $x = \frac{R-\mu_R}{\mu_R}$, a unique distribution with a known variance.

(b) Generalized Probability Distribution

The validity of extrapolating the "t" distribution beyond $x = 0.15$ is of little practical importance since under any of the service load spectra the probability of failure in the region $x > 0.15$ is negligible.

For the critical range $-1.0 \leq x < -0.15$, however, extrapolation of the "t" distribution proves unacceptable. The probability density function is finite for structures of zero strength ($x = -1.0$), which is physically unrealistic; it predicts, moreover, a high failure rate for structures of negligible ultimate strength when combined with typical load spectra.

This is referred to further in Section 4 where it is shown that with the exponential gust load spectrum a "t" distribution of structural resistance produces a spurious increase in the marginal density function of structural resistance

$$p(R) = p_R(R) [1 - P_S(R)]$$

for values of structural resistance less than 80% of the mean value $\left(x = \frac{R - \mu_R}{\mu_R} < -0.2\right)$.

This problem can be overcome by truncating the "t" distribution of structural resistance at a suitable value, on the quite justifiable assumption that structures of lower strength will be eliminated by inspection during manufacture. It is known from experience that the rare occurrences of ultimate failure in service do not arise because of structures having extraordinarily low strength but rather because structures of adequate strength encounter extreme loading conditions.

Fundamentally, however, it is desirable to apply the reliability approach over the whole range of possible structural resistance and this also makes it possible to assess the various parameters.

However, until further data on ultimate strength are available, the behavior of the distribution near the extreme values can be based only on physical reasoning.

The probability distribution of the ultimate stress at failure in metals can be approximated by a log-normal distribution⁹ or, in fact, for the low variances that apply, a simple normal distribution. The ultimate failure of structures is further dependent on the load eccentricity in the critical members, represented by $e^2 = z_1^2 + z_2^2 + z_3^2$ where z_1, z_2, z_3 are the components of eccentricity parallel to any three fixed perpendicular axes. If the deviations z_1, z_2, z_3 are assumed to be normally distributed about zero, e^2 is therefore an χ^2 variate with three degrees of freedom.

This gives some physical explanation of why the structural resistance appears as a "t" statistic, defined by a normal variate (the distribution of ultimate stress) divided by the square root of an χ^2 variate with 3 degrees of freedom (the distribution of load eccentricity "e"). It represents the effect of load eccentricity, inducing bending stresses which add to (or subtract from) the direct stress in members at the critical point.

The allowable eccentricities due to lack of straightness in members, inexact location of bolt and rivet holes,

etc., will be held within fixed limits by the normal production standard. Beyond these limits it seems reasonable to assume a log-normal distribution of strength, representing the validity in ultimate strength of the material itself.

Therefore extrapolation has been done, using a log-normal distribution with mean at $x = 0$ and variance selected to make it continuous with the "t" distribution at $x = -0.2$.

This leads to the following distribution of structural resistance:

$$\begin{aligned}
 p(x)dx &= \frac{2\sigma_X^3}{\pi(\sigma_X^2 + x^2)^2} & -0.2 \leq x < \infty \\
 & & (3.6) \\
 &= \frac{4.6955}{(x+1)} e^{-\frac{(\log_{10} \overline{x+1})^2}{.002723}} & -1 \leq x \leq -0.2
 \end{aligned}$$

$$\text{with } \sigma_x = 0.05638$$

In applying the reliability function it is often an advantage to have an algebraic expression for the probability distribution of $x, \left(\int_{-1}^x p(u).du \right)$. While this exists for the "t" distribution it does not exist for the log-normal distribution and a polynomial approximation is therefore proposed as an alternative:

$$p(x)dx = 0.6096 (x + 1)^{10.3} \quad -1 \leq x \leq -0.2 \quad (3.7)$$

(c) Probability Distribution for Symmetric Structures

Some aircraft structures, such as mainplanes, are usually symmetric in that they consist of two nominally identical halves. Ultimate failure of the structure then constitutes failure of the weaker of two members from the population. The data in the foregoing analysis are from asymmetric tests or from symmetric tests on asymmetric structures in which failure always occurs on one side, which is also nominally the weaker.

Some data available on symmetric structures have been analyzed and indicate that the strength of the two halves is not independent but is highly correlated. The preliminary conclusion is that it is more accurate to apply the foregoing distribution to the whole structure on the assumption of complete correlation (i.e., both halves always of identical strength) than it is to apply the distribution for the lesser of two independent ("t" distributed) variates (i.e., both halves selected at random from the population).

The physical significance of this is that in production two equally high (or low) strength structures are produced at the same time and assembled. To determine the precise degree of correlation (if a unique value exists) will require further data from symmetric structures.

The effect of ultimate failures in different areas of the same structure is represented in the data since some types of structure showed both tension and compression failures at the ultimate bending moment. However, this effect is rather small in uncracked structures since, because of general yielding, the load distribution at ultimate failure is characteristic and is consistently reproduced.

4. ULTIMATE STRENGTH ANALYSIS

Consider a load S chosen at random from the population of service loads and applied to a structure of resistance R chosen at random from the population of structures. Following the theory developed by Freudenthal¹ the probability of failure is given by

$$P_F = \iint_{\{R \leq S\}} p_R(R) p_S(S) dR dS \quad (4.1)$$

where R and S are assumed to be independent and the integration is carried out over the region $R \leq S$ (i.e., the quadrant bounded by $R = 0$ and $R = S$ as shown in Fig. 1).

(a) Reliability Equations

Integrating (4.1) with respect to R and S over the region $R \leq S$

$$\begin{aligned} P_F &= \int_0^{\infty} \int_R^{\infty} p_R(R) p_S(S) dS dR \\ &= \int_0^{\infty} p_R(R) [1 - P_S(R)] dR \\ &= \int_0^{\infty} p_R(R) \bar{F}_S(R) dR \end{aligned} \quad (4.2)$$

The marginal density function of the joint distribution (4.2) within the limits $0 < R < S$ is:

$$p(R) = p_R(R) \bar{F}_S(R)$$

Multiplication by dR produces the probability that failure will occur in structures with resistance in the interval R to $R + dR$. This is evident from first principles since $p_R(R)dR$ is the probability of structures having resistance R to $R + dR$ and $\bar{F}_S(R)$ is the probability of exceeding a service load R . Hence, assuming independence

$$p_R(R) \cdot dR \cdot \bar{F}_S(R) = P_r$$

where P_r denotes failure of structures with resistance R to $R + dR$.

The probability of failure of a structure with resistance less than \hat{R} is therefore

$$P_F(R < \hat{R}) = \int_0^{\hat{R}} p_R(R) \bar{F}_S(R) \cdot dR \quad (4.3)$$

Changing the order of integration Eq. (4.1) may be written

$$P_F = \int_0^{\infty} dS \int_0^{R=S} p_S(S) \cdot p_R(R) \cdot dR = \int_0^{\infty} p_S(S) P_R(S) \cdot dS \quad (4.4)$$

The marginal density function of the joint distribution (4.2) within the limits $R < S < \infty$

$$p(S) = p_S(S) P_R(S)$$

and

$$p(S).dS = P_r$$

where P_r is the failure of structures under a service loads. This also depends on the assumed independence of R and S since $p_R(S)dS$ is the probability of occurrence of a service load between S and $S + dS$ and $P_R(S)$ is the probability of a structure with resistance less than S . The combination of these two events constitutes failure under a service load between S and $S + dS$. Hence the failure P_r under a service load S may be expressed as

$$P_r = p_S(S) P_R(S).dS$$

The probability of failure under a service load less than \hat{S} is

$$P_F(S < \hat{S}) = \int_0^{\hat{S}} p_S(S) P_R(S).dS \quad (4.5)$$

The relation between $P_F(R < \hat{R})$ and $P_F(S < \hat{S})$ is readily obtained by referring to Fig. 8 where the respective areas of integration are shown.

$$P_F(R < \hat{R}) = P_F(S < \hat{R}) + P_R(\hat{R}).\bar{F}_S(\hat{R}) \quad (4.6)$$

which is obtained by the following consideration of first principles.

$$\begin{aligned}
P_R \{ \text{failure of structure with } R \leq \hat{R} \} &= \\
&= P_R \{ \text{failure with } R \leq \hat{R} \text{ and } S \leq \hat{R} \} + \\
&\quad P_R \{ \text{failure with } R \leq \hat{R} \text{ and } S < \hat{R} \} \\
&= P_F \{ S < \hat{R} \} + P_R \{ R \leq \hat{R} \} \cdot P_R \{ S > \hat{R} \} \\
&= P_F \{ S < \hat{R} \} + P_R (\hat{R}) \cdot \bar{F}_S (\hat{R})
\end{aligned}$$

Either of the alternative forms for P_F in Eqs. (4.2) and (4.4) may be adopted depending on which one may be more easily integrated. The functions $P_F(R < \hat{R})$ and $P_F(S < \hat{S})$ are of interest in investigating the values of R and S at failure.

Making use of the distribution function P_x for the relative variation in structural resistance x developed in Section 3 and the probability distributions \bar{F}_u, \bar{F}_n for exceedance of service loads in various operations listed in Section 2, the functions $P_F\{R < \hat{R}\}$ and $P_F\{S < \hat{S}\}$ may be expressed as follows.

$$\begin{aligned}
\text{Taking } P_F\{R < \hat{R}\} \text{ with } x &= \frac{R}{\mu R} - 1 \text{ and } X = \frac{\hat{R}}{\mu R} - 1 \\
P_F\{R < \hat{R}\} &= P_F\{x < X\} = \int_0^{\hat{R}} P_R(R) \bar{F}_S(R) dR \\
&= \int_0^{\hat{R}} p_x(x) \frac{dx}{dR} \bar{F}_u(U_R) \cdot dR \quad (4.7) \\
&= \int_{-1}^X p_x(x) \bar{F}_u(U_R) \cdot dx = \int_{-1}^X p_x(x) \bar{F}_n(\Delta n_R) \cdot dx
\end{aligned}$$

U_R or Δn_R may be expressed in terms of x using the design conditions as shown in Eq. (4.2) and the integral may then be evaluated.

Considering $P_F\{S < \hat{S}\}$ and defining $y = \frac{S}{\mu_R} - 1$ with $Y = \frac{\hat{S}}{\mu_R} - 1$ it follows that

$$\begin{aligned}
 P_F\{S < \hat{S}\} &= P_F\{Y < Y\} = \int_0^{\hat{S}} p_S(S) P_R(S) .dS \\
 &= \int_0^{\hat{S}} p_Y(y) \frac{dy}{dS} P_X\left(\frac{S}{\mu_R} - 1\right) .dS \\
 &= \int_{-1}^Y p_Y(y) P_X(y) .dy \qquad (4.8) \\
 &= \int_{-1}^Y \left\{ p_U(U_S) \frac{dU_S}{dy} \right\} P_X(y) .dy \\
 &= \int_{-1}^Y \left\{ p_n(n_S) \frac{dn_S}{dy} \right\} P_X(y) .dy
 \end{aligned}$$

Here again n_S and $\frac{dn_S}{dy}$ or U_S and $\frac{dU_S}{dy}$ may be expressed in terms of y using the design conditions and the integral can therefore be evaluated.

(b) Design Conditions

In formulating the design conditions it is assumed that: (1) The distribution of the applied load remains constant and its magnitude is proportional to the acceleration produced at the center of gravity; and (2) Changes in air loads due to gusts are proportional to the gust velocity.

The following notation will be employed in the discussion of design conditions:

- W actual operating weight under different conditions
- n acceleration at the center of gravity due to the applied load
- n_o acceleration at the center of gravity in straight and level flight (normally $n_o = +1$ for positive loading case and $n_o = -1$ for negative loading case).
- Δn acceleration produced by a change in the applied load, i.e., $n = n_o + \Delta n$.
- K_n $\frac{\Delta n}{U}$ (where U is the gust velocity), a gust sensitivity factor
- p probability that a specified minimum strength R_p is not exceeded in the population of structural resistance R, i.e., $p = P_r \{R < R_p\}$.
- q probability that a specified maximum load S_q is exceeded in the population of service loads S, i.e., $q = P_r \{S \geq S_q\}$
- $\alpha_{R,p}$ $\frac{R_p}{\mu_R}$, the ratio of the specified minimum strength to the mean structural resistance μ_R
- $\bar{v}_{p,q}$ a safety factor defined by $\bar{v} = \frac{R_p}{S_q} = \frac{\alpha_{R,p} \mu_R}{S_q}$

S_q has been taken in all cases as the value specified in current design requirements. Two values of R_p have been considered in order to apply the design philosophy of Reference 1.

To simplify the notation no subscripts are used on \bar{v} in the following equations, but \bar{v} is always shown associated with a corresponding value of p (or $\alpha_{R,p}$).

The values of p considered are:

(i) $p = 0.1$ based on the assumption that R_p is the structural resistance corresponding to the specified minimum values of the material properties. It has been shown by Freudenthal⁹ from extensive test data on small specimens that approximately 10% of the specimens in a large sample give values below the specification minimum. This indicates that a value of $p = 0.1$ is reasonable; the corresponding value of $\alpha_{R,p}$ based on the "t" distribution in (3.6) is $\alpha_{R,p} = 0.947$.

(ii) $p = 0.5$ on the assumption that R_p is equal to the mean structural resistance μ_R ($\alpha_{R,p} = 1.0$). This is assumed to be the condition relevant to present aircraft design standards, since in current design the ultimate failing load as determined in the usual single test to destruction exceeds the design ultimate load by a negligible margin.

The current safety factor on aircraft design loads is 1.5 and hence $\bar{v} = 1.5$, $p = 0.5$ is the equivalent condition for comparison with service conditions.

Considering an upward load applied to the structure

$$R = W \cdot n_R = W(n_o + \Delta n_R)$$

$$R_p = \mu_R \cdot d_{R,p} = \bar{v} W (n_o + \Delta n_q)$$

$$\therefore x = \frac{R}{R_p} - 1 = \frac{R \cdot \alpha_{R,p}}{R_p} - 1 = \frac{(n_o + \Delta n_R) \alpha_{R,p}}{(n_o + \Delta n_q) \bar{v}} - 1 \quad (4.9)$$

with $\Delta n_R \geq 0$ and hence $x \geq \frac{\alpha_{R,p} \cdot n_o}{n_q \cdot \bar{v}} - 1$. Hence

$$\Delta n_R = \frac{(x + 1)(n_o + \Delta n_q) \bar{v}}{\alpha_{R,p}} - n_o; \quad x \geq \frac{\alpha_{R,p} \cdot n_o}{n_q \bar{v}} - 1 \quad (4.10)$$

or

$$U_R = \frac{\Delta n_R}{K_n} = \frac{(x + 1)(n_o + K_n U_q) \bar{v}}{\alpha_{R,p} K_n} - \frac{n_o}{K_n}; \quad x \geq \frac{\alpha_{R,p} \cdot n_o}{K_n U_q \bar{v}} - 1 \quad (4.11)$$

Substitution of these values in (4.7) transforms

$\bar{F}_n(\Delta n_R)$ or $\bar{F}_U(U_R)$ to a function of x with the lower

limit of integration taken at $x = \frac{\alpha_{R,p} \cdot n_o}{n_q \bar{v}} - 1$ or

$x = \frac{\alpha_{R,p} \cdot n_o}{K_n U_q \bar{v}} - 1$. For a downward load changing the sign of

n_o produces

$$\Delta n_R = \frac{(x + 1)(\Delta n_q - n_o) \bar{v}}{\alpha_{R,p}} + n_o \quad (4.12)$$

or

$$U_R = \frac{(x + 1)(K_n U_q - n_o) \bar{v}}{\alpha_{R,p} K_n} + \frac{n_o}{K_n} \quad (4.13)$$

with Δn_R and U_R now necessarily greater than or equal to zero for $x \geq -1$.

For a lateral load $n_o = 0$ and therefore

$$\Delta n_R = \frac{(x + 1) \Delta n_q \bar{v}}{\alpha_{R,p}} \quad (4.14)$$

$$U_R = \frac{(x + 1) U_q \bar{v}}{\alpha_{R,p}} \quad (4.15)$$

With $\Delta n_R \geq 0$ and $U_R \geq 0$ and provided that $x \geq -1$,

$P_F\{R < \hat{R}\}$ can therefore be evaluated from (4.7) by substituting for Δn_R or U_R according to the case considered.

Similarly for $R_F\{S < \hat{S}\} = P_F\{y < Y\}$ with

$$S = W(n_o + \Delta n_S) = W(n_o + K_n U_S)$$

$$y = \frac{S}{\mu_R} - 1 = \frac{(n_o + \Delta n_S) \alpha_{R,p}}{(n_o + \Delta n_q) \bar{v}} - 1 \quad (4.16)$$

by comparison of (4.16) and (4.9) it follows that Δn_S and $U_S = \frac{\Delta n_S}{K_n}$ are obtained directly from the corresponding expressions for Δn_R and U_R by replacing x by y .

For an upward load

$$\Delta n_S = \frac{(y + 1) (n_o + \Delta n_q) \bar{v}}{\alpha_{R,p}} - n_o; \quad y \geq \frac{\alpha_{R,p} n_o}{n_q \bar{v}} - 1 \quad (4.17)$$

$$U_S = \frac{(x + 1) (n_o + K_n U_q) \bar{v}}{\alpha_{R,p}} - \frac{n_o}{K} ; \quad y \geq \frac{\alpha_{R,p} n_o}{K_n U_q \bar{v}} - 1 \quad (4.18)$$

For a downward load:

$$\Delta n_S = \frac{(y+1)(\Delta n_q - n_o)\bar{v}}{\alpha_{R,p}} + n_o \quad (4.19)$$

$$U_S = \frac{(y+1)(K_n U_q - n_o)\bar{v}}{\alpha_{R,p} K_n} + \frac{n_o}{K_n} \quad (4.20)$$

For a lateral load:

$$\Delta n_S = \frac{(y+1)\Delta n_q \bar{v}}{\alpha_{R,p}} \quad (4.21)$$

$$U_S = \frac{(y+1)U_q \bar{v}}{\alpha_{R,p}} \quad (4.22)$$

(c) Influence of the Design Parameters

On the basis of the preceding equations the influence of the relevant parameters on the probability of failure in civil and military aircraft structures may be investigated.

(i) Civil Transport Aircraft

Considering Civil Airworthiness Requirements¹⁰ the feasible range of the parameters may be established as follows.

For positive loads: $\mu_R \geq (1 + 1.5)\bar{v} W$ Maneuver case

$\mu_R \geq (1 + K_n U_q)\bar{v} W$ Gust case

For negative loads: $\mu_R \geq (2 - 1)\bar{v} W$ Maneuver case

$\mu_R \geq (K_n U_q - 1)\bar{v} W$ Gust case

Since the gust loads in civil aircraft are always relatively severe, the gust critical condition will be considered next. Denoting the applied load in the steady flight condition by $n_o W$

$$\mu_R = \alpha_{R,p} R_p \geq (K_n U_q + n_o) \bar{v} W$$

with $K_n U_q \geq 1.5$ for upward loads ($n_o = +1$)

$K_n U_q \geq 2$ for downward loads ($n_o = -1$)

Minimum values are thereby established for the design parameter K_n . The influence of K_n on the probability of failure is indicated by U_o , the gust velocity corresponding to the average structural resistance μ_R .

Setting $x = 0$ in (4.11)

$$U_o = \frac{\bar{v} U_q}{\alpha_{R,p}} + \frac{n_o}{K_n} \left(\frac{\bar{v}}{\alpha_{R,p}} - 1 \right)$$

With $n_o = -1$, U_o increases with increasing K_n and the minimum value of K_n ($K_n = \frac{2}{U_q}$) is therefore critical for downward loads (since $\bar{v} \geq 1$). With $n_o = +1$, U_o decreases with increasing K_n and the upper limit of K_n is critical for failure in the up-load case.

In any civil aircraft design the maximum design load is never likely to exceed $4W$. Considering this as an upper limit

$$(K_n U_q + 1) \bar{v} W < \mu_R < 4 v W$$

$$\therefore K_n U_q < 3$$

Realistic values for the design parameter K_n can therefore be expressed as

$$\frac{1.5}{U_q} \leq K_n \leq \frac{3}{U_q}$$

Referring to (4.11), the effect of varying the parameters \bar{v} and $\alpha_{R,p}$ has been investigated for various values of K_n using the thunderstorm gust load distribution from Section 2a(i). The influence of K_n has been investigated for the normal value of $\bar{v} = 1.5$ with $p = 0.1$ and 0.5 . For comparison a calculation for a particular case has been made using the gust load distribution of Section 2a(ii). An outline of these calculations is shown in Table 5 where the values of the parameters are listed with the reliability equations.

(ii) Military Aircraft

The probability of failure under gust loads is analogous to that investigated for civil transport aircraft in (i). However, for fighter aircraft the maneuver load spectrum is quite distinct from the exponential gust load spectrum.

The semi-normal probability distribution for maneuver loads, given in Section 2b(i), is not readily integrated and the form of the reliability equation (4.8) has therefore been adopted, using the integrable form of $p(x)$ in (3.7) with $p(\Delta n_S)$.

From Eq. (4.17)

$$\Delta n_S = \frac{(y + 1)(n_o + \Delta n_q)\bar{v}}{\alpha_{R,p}} - n_o$$

Hence $p(\Delta n_S)$ may be transformed into a function of y , introducing the parameters

$$n_q = 1 + \Delta n_q^*, \quad \bar{v}, \quad \alpha_{R,p} \quad \text{and} \quad \sigma_n \quad \text{with} \quad n_o = +1.$$

The effect of the specification parameters \bar{v} and $\alpha_{R,p}$ has been investigated for typical values of n_q and σ_n . The effect of the service load parameter σ_n has also been investigated taking $n_q = 8 \frac{2}{3}$ and $7 \frac{1}{3}$ corresponding to the FI and FII categories in military specification MIL-A-8861(ASG) for the standard design values $\bar{v} = 1.5$, $\alpha_{R,p} = 1.0$. The cases calculated are listed with the relevant values of the parameters in Table 4.

(d) Comparison with Service Conditions

To test the application of the foregoing theory, the probability of failure has been predicted for specific cases

in which data on the failure rate have been obtained from service records.

(i) Civil Transports

Accident statistics for United States and United Kingdom civil transport aircraft in the post-war period have been obtained to establish an overall failure rate per hour.^{11,12} These data are compared in Table 5 with the results predicted by theory for both the thunderstorm gust data and the general gust data (Section 2a).

Design values $\bar{v} = 1.5$ and $\alpha_{R,p} = 1.0$ have been taken and the combined failure rates under up-gust and down-gust are presented for a series of values of K_n for the thunderstorm gust spectrum.

(ii) Heavy Bombers

Data from a large fleet of heavy bombers, in both high- and low-level operations, are shown in Table 5. Also presented for comparison are failure rates predicted by the reliability equation (3.7) for the following cases.

(1) Lateral gusts for low- and high-level operation, based on the ultimate gust velocity U_0 for the design operating conditions .

(2) Vertical accelerations (including gusts and maneuvers) for the average operating conditions of the fleet

at both high and low level. The particular service load data for the case are shown in Fig. 6.

In (1) no cases of wing bending failures have been reported so that only a lower limit for the failure rate can be established from the service operations.

In (2) the operating conditions at both high and low level are substantially different from design operating conditions. The value of U_0 taken in the calculations, although based on experiment, is therefore too high for the low-level operation, and too low for the high-level conditions.

This preliminary estimate of the failure rate, therefore, gives no more than an approximate indication.

(iii) Fighter Aircraft

Data from a large fleet of fighter aircraft in both training and combat operations are shown in Table 5. In this case the ultimate load at failure has been determined on a number of specimens and data taken on V-g recorders during training operations are also available.

The failure rate has been predicted by the reliability equation (4.8) using the service data applying to the fleet.

5. FATIGUE STRENGTH ANALYSIS

Data on the fatigue performance in service of the three classes of aircraft being considered (i.e., civil, bomber and fighter) are included in Table 5. These have been combined with whatever fatigue information could be obtained on the structure to determine the risk of fatigue failure $r_F(N)$. Following the proposals in Reference 1 the fatigue sensitivity factor $\left[f = \frac{r_F(N)}{r_u(N)} \right]$ has been obtained using the results from the ultimate strength analysis in Section 4.

(a) Civil Aircraft

Data from United States Air Carrier operations over the period 1946-1960 have been analyzed¹¹ and are presented in Table 5. Similar data for British aircraft in the period 1948-1956 have been reproduced from Reference 12. The total flying hours were not given in this source but an approximate figure of 2×10^6 hours per year has been estimated indirectly and has been adopted as sufficiently accurate for the present purpose.

The average failure rate per hour has been calculated for both fatigue and ultimate load failure. The

United States and British figures show reasonable agreement and have been combined to give an average estimate. The calculation of a uniform failure rate is valid for ultimate failure since it is regarded as due to random causes. The failure rate in fatigue, however, increases during the service life of each particular aircraft and the average figure gives only a gross estimate. It has been multiplied by 2 on the assumption of a linearly increasing rate to give an approximate figure. At the very low probabilities of failure involved the risk of failure is virtually the same as the failure rate.

An estimate of the fatigue sensitivity of $(N^*) =$

$\frac{P_F}{P_U} = \frac{r_F}{r_U}$ has thus been made, giving the overall fatigue sensitivity for the whole population of aircraft at the end of the average service life.

(b) Heavy Bomber Aircraft

A sample of 40 aircraft in the fleet has been considered, assuming that each craft was operated under a common spectrum of service loads. All aircraft were inspected over a period and initial fatigue failures were noted. At the same time the structure was modified in the fatigue critical area whether cracks were present or not.

From the data listed in Table 6 it can be seen that 19 aircraft were modified before initial failure, and the data therefore include 19 arbitrarily censored values of service life. Assuming a log-normal distribution of life, the mean and variance have been estimated from the following maximum likelihood equations, applying to a sample of n with $n-k$ censored values:¹⁵

$$\mu_Z = \bar{Z} + \frac{\sigma_Z}{k} \sum_{j=1}^{n-k} A(v_j) \quad (5.1)$$

$$\sigma_Z^2 = \frac{\sum_{i=1}^k (Z_i - \mu_Z)^2}{n-k - \sum_{j=1} [v_j A(v_j)]} \quad (5.2)$$

where $Z_i = \log N_i$ for $i = 1, \dots, k$.

$$v_j = \frac{Z_j - \mu_Z}{\sigma_Z}$$

$$A(v_j) = \frac{e^{-1/2 v_j^2}}{\int_{v_j}^{\infty} e^{-1/2 t^2} dt}$$

These have yielded values $\mu_Z = 3.2948$, $\sigma_Z^2 = 0.005348$, giving $\mu_N = 1970$ hours with $\sigma_Z = 0.0731$. The corresponding log normal distribution has been drawn in Fig. 9 giving the probability of failure $P(N)$ at N hours. The risk

function associated with $P(N)$ is

$$r_F(N) = \frac{\log e \left(e^{\frac{(\log N - \mu_Z)^2}{2\sigma_Z^2}} \right)}{N \cdot \sigma_Z \int_{\frac{\log N - \mu_Z}{\sigma_Z}}^{\infty} e^{-1/2 t^2} dt} \quad (5.3)$$

A plot of the relative frequency of the individual data points has also been made by employing the risk function.

Assume that

m_N = number of structures remaining at life N

M_N = number of structures in the original population which would give an expected number m_N left at N

Δm_N = number of structures that fail in fatigue during a small interval N to $N + \Delta N$ during which no values are censored (M_N constant).

The model postulated is that censored values are removed at N , and no censoring takes place until $N + \Delta N$ when further censored values are suddenly removed and so on.

Now $L(N) = \frac{m_N}{M_N}$ but M_N is not known from the data

$$p(N) = - \frac{\Delta L(N)}{\Delta N} = \frac{\Delta m_N}{M_N} / \Delta N$$

$$r(N) = \frac{p(N)}{L(N)} = \frac{\Delta m_N}{M_N \cdot \Delta N} / \frac{m_N}{M_N} = \frac{\Delta m_N}{m_N \cdot \Delta N}$$

$r(N)$ is therefore the only function independent of M_N .

Taking the relation $L(N) = e^{-\int_0^N e(t) \cdot dt}$

where

$$\begin{aligned}
 \int_0^N r(t) \cdot dt &= \sum_{i=1}^r r(t_i) \cdot \Delta t_i \\
 &= \sum_{i=1}^r \frac{\Delta m_{t_i}}{m_{t_i} \cdot \Delta t_i} \Delta t_i \\
 &= \sum_{i=1}^r \frac{\Delta m_{t_i}}{m_{t_i}}
 \end{aligned}$$

Δm_{t_i} is the number of structures that fail in an interval Δt_i ; since Δt_i is arbitrary the intervals may be selected such that $\Delta m_{t_i} = 1$. Hence

$$L(N_{tr}) = e^{-\sum_{i=1}^r \frac{1}{m_{tr}}} \quad (5.4)$$

where N_{tr} is the life to fatigue failure of the m_{tr} , the structure to be removed from the population.

The frequency distribution for the 21 values of fatigue life in Table 6 has been plotted in Fig. 19 from which it will be seen that median value agrees very closely with the log normal distribution but that the variance is considerably lower. A log normal distribution with a standard deviation $S(\log N) = .036$ has been drawn to show a comparison with the frequency distribution.

From the extensive crack propagation data available on distributed member two-spar structures, a crack propagation period of 60% of the total life seems realistic for the well-defined initial failure considered here. This provides an approximate estimate of 5,000 hours for the life to final failure.

(c) Fighter Aircraft

A large percentage of the fighter fleet was inspected and fatigue cracks of varying extent were found in a number of aircraft. These failure data have been corrected on the basis of known crack propagation rates to correspond to a typical initial failure for all cases.

From these data a life of 500 hours with a standard deviation of 0.186 is obtained, which is in reasonable agreement with test results.

There is no record of complete structural failure in service due to fatigue but it is known from actual test data that final failure occurs in another part of the structure. The crack propagation time is approximately 20% of the total life and it is therefore not surprising that no initial failures were found in this region. The fatigue life from representative test data is 3,100 hours with a standard deviation of .073.¹³

It will be noted that the standard deviation is virtually the same as that for the bomber and is in agreement with other data on the standard deviation at relatively short fatigue lives as quoted by Patching.¹⁴

(d) Calculation of Fatigue Sensitivity

The risk function $r_F(N)$, given in (5.3) can be transposed into a non-dimensional form as follows:

$$r_{F \cdot \mu_N} = \frac{\log_{10} e \cdot e^{-\frac{\left(\log \frac{N}{\mu_N}\right)^2}{2\sigma_Z^2}}}{(N/\mu_N) \cdot \sigma_Z \int_{\log N/\mu_N}^{\infty} e^{-1/2 t^2} \cdot dt}$$

This gives $(r_{F \cdot \mu_N})$ as a function of $\frac{N}{\mu_N}$ which applies to all log-normal distributions of the same variance σ_Z^2 . The function has been plotted for $\sigma_Z = .073$ in Fig. 20 and used to calculate the fatigue sensitivity $r_F(N)$ at certain lives as shown in Table 6. In particular the life N_0 for equal risk of ultimate and fatigue failure has been estimated.

6. DISCUSSION OF RESULTS

The results obtained in Sections 4 and 5 are presented in Tables 4 and 5 and in Figures 9 to 19.

(a) Ultimate Failure

In Fig. 9 the probability of failure $P_F(X)$ under the thunderstorm gust distribution (Case 2 in Table 4b) is shown for various forms of the distribution of relative structural resistance x . The three alternative forms for the distribution of x discussed in Section 3 (viz. the truncated "t," the truncated "t" with polynomial form below $x = -0.15$, and the truncated "t" with log-normal form below $x = -0.15$) show good agreement for the total probability of failure P_F . However, the form of the lower tail of the distribution has a very marked effect on the probability of failure as is shown by the difference between the high order polynomial and log-normal distributions.

This effect is also pronounced with the maneuver load spectrum as shown in Fig. 16 where the probability of failure below a given structural resistance $P_F(X)$ and the probability of failure below a given load $P_F(Y)$ are both compared. In fact, for most cases the maneuver load spectrum is much

more sensitive in this respect and therefore the probabilities of failure for fighter aircraft have been truncated at $x = -0.25$.

The curves also show that the great majority of structural failures are at structural resistances near the mean. This indicates that the scatter in structural resistance at present achieved in production should not seriously increase the risk of failure which would, therefore, be decisively determined by the load spectrum. The comparison between the total probabilities of failure predicted by the invariate case and the probability distributions substantiates this view.

However, further data are needed to investigate the behavior of the distribution of structural resistance at the low extreme values. It should also be noted that the probability of failure is very sensitive to changes in the mean. This is shown by the curves of $P_F(X)$ for various values of the design parameters \bar{v} and p in Figs. 10 to 13 applying to the thunderstorm gust distribution.

The effect is clearly shown in Fig. 15 where the total probability of failure has been plotted as a function of \bar{v} for the thunderstorm gust and maneuver load cases. The slope of the curves near $\bar{v} = 1.5$ shows the effect of a variation

in the mean structural resistance. Bearing in mind that P_F is plotted on a logarithmic scale, the effect is very marked particularly for the maneuver load spectrum.

This suggests that the probability of failure in structures developing fatigue cracks may be very much greater than anticipated. However, reliable data on the relationship between structural resistance and crack length in the general case are needed to investigate this important question.

The influence of the gust sensitivity K_n is shown in Fig. 14 for the thunderstorm gust distribution. The effect on the probability of failure is not appreciable except in the critical downgust case at low values of K_n . However, there is a lower limit of $K_n = .0303$ applied by the Airworthiness Requirements in this case as discussed in Section 4(b).

For fighter aircraft the effect of the mission parameter σ_n is shown in Fig. 17. In conjunction with the values of σ_n listed in Table 1, this indicates the very great influence that the type of mission has on the probability of failure. In changing from the "general mission" role ($\sigma_n = 1.27$) to the severe ground attack ($\sigma_n = 1.97$) the probability of failure per load application is increased by five orders of magnitude.

In Fig. 18 the failure rates per hour of the three types of aircraft (civil transport, bomber and fighter) are compared for representative missions.

The comparison between the failure rate experienced in service with that predicted for average operating conditions is presented in Table 5(a).

For civil transports, an average cruising speed of 200 mph and operating height of 20,000 feet has been assumed representative of the period considered. The agreement between the failure rates per hour on this basis is very good.

The comparison for the bomber in the case of vertical acceleration is limited by the relatively low total hours accumulated by the fleet. The failure rate predicted for lateral gusts does not show agreement with that obtained from service records. It is considered that this is mainly due to an inadequate estimate at this stage of the ultimate gust velocity U_0 corresponding to the particular operating conditions.

The failure rate predicted for the fighter is based on the maximum operating conditions. Since the operating weight was usually less than the maximum allowable a failure rate corresponding to $r_u = 11$ (all upweight = 85% maximum) has also been presented. The comparison of the latter figure

with the failure rate recorded in service is quite reasonable. This is considered a realistic comparison, especially as in only one of the three accidents reported was the take-off weight equal to that allowable.

(b) Fatigue Failure

Fatigue data for the three categories -- civil transport, bomber and fighter -- are presented in Table 5(b).

(i) Civil Transport

No data referring to particular aircraft have been analyzed but comparison of the service data in 4(a) and 4(b) indicates that the ultimate failure rate p_u is about 3/4 of the failure rate for fatigue p_F at the end of the average service life N^* . Considering the large number of hours involved and the close agreement between the overall figures in this table, the factor is regarded as significant.

Accepting the assumptions of a constant value of p_u and a linearly increasing value for p_F throughout the life, this infers that

$$\frac{p_F(N_o)}{p_U} = \frac{r_F(N_o)}{r_u(N_o)} = 1$$

at 3/4 of the average service life N^* .

(ii) Heavy Bomber

The fatigue life to initial failure has been assumed to have a log normal distribution with a mean $\mu_N = 1,970$ hours and a standard deviation $S(\log N) = .073$ as estimated by maximum likelihood. The plot of the observed frequency points in Fig. 19, using the method developed in Section 5, shows good agreement with the median of the proposed distribution. However, it is considered that these results suffer from the fact that the inspection intervals have become effectively shorter as the total hours of the fleet increased. Even small variations in the extent of the detected cracks introduce a bias under this procedure.

The rather low variance for an initial fatigue failure obtained by maximum likelihood may be due to this effect also, but the overall influence on the mean and standard deviation should nevertheless be much reduced.

Calculation of the fatigue sensitivity has been carried out as described in Section 5(d). The life N_0 for equal risks of ultimate and initial fatigue failure has been estimated as 960 hours. This value is relatively short for the service life of a bomber but it is influenced first by the fact that initial fatigue failure has been considered and second by the very severe load spectrum.

(iii) Fighter

The life and standard deviation given in Section 5 are considered to be very well based and since the value of standard deviation is appropriate the curve in Fig. 20 has again been used to deduce the values of fatigue sensitivity shown in Table 6. The value of N_0 in this case is 1,900 hours which is again relatively low, especially considering that a number of these aircraft had exceeded a service life of 2,000 hours.

7. CONCLUSIONS

(i) The reliability theory has predicted probabilities of ultimate load failure in good agreement with those recorded in service for civil transports, a typical bomber, and a typical fighter aircraft.

(ii) The variability in the ultimate strength of structures under present production standards is satisfactory, although probably marginal.

(iii) The failure rate is very sensitive to the mean structural resistance of the population, particularly under the maneuver load spectrum.

(iv) In view of (iii) the structural reliability of airframes containing even small fatigue cracks requires close investigation when the fail-safe principle is invoked.

(v) The failure rate is greatly influenced by the design parameter \bar{v} for all the service load spectra considered. Under the gust load spectrum the failure rate increases with an increase in the gust sensitivity factor

K_n in the critical downgust case, but decreases with increasing K_n in the upgust case.

Under the maneuver load spectrum a variation in the failure rate of 5 orders of magnitude is predicted, according to the type of mission considered.

(vi) The fatigue sensitivity factor $f(N^*) = \frac{r_F(N^*)}{r_u(N^*)}$ varies greatly according to the value taken for the service life N^* with respect to the mean fatigue life. A useful and more stable indication of fatigue sensitivity is the life N_0 at which the risks of ultimate load and fatigue failure are equal [$f(N_0) = 1$].

(vii) For airframes in the three categories considered, civil transport, bomber and fighter, the risk of fatigue failure appreciably exceeds the risk of ultimate load failure at the end of the normal service life N^* .

LIST OF REFERENCES

1. Freudenthal, A. M. Fatigue Sensitivity and Reliability of Mechanical Systems, especially Aircraft Structures. WADD Technical Report 611-53. July 1961.
2. Pugsley, A. G. A Philosophy of Aeroplane Strength Factors. Aeronautical Research Council Reports and Memoranda No. 1906. February 1945.
3. Atkinson, R. J. Permissible Design Values and Variability Test Factors. Aeronautical Research Council Reports and Memoranda No. 2877. July 1950.
4. Lundberg, B. "The Quantitative Statistical Approach to the Aircraft Fatigue Problem." Proceedings of Symposium on Full-Scale Fatigue Testing of Aircraft Structures. London: Pergamon Press (1961), p. 393.
5. Tolefson, H. B. Summary of Derived Gust Velocities Obtained from Measurements within Thunderstorms. NACA Report 1285.
6. McDougal, R. L., Coleman, T. L. and Smith. P. L. NACA Research Memorandum L53G15a. Washington, 1953.
7. Royal Aeronautical Society. Fatigue Data Sheets L.01. Average Gust Frequencies. June 1958.
8. Whitford, D. K. Service Loads Recording Program (Heavy Bomber) - Lateral Loads. Project Report E.C.P. 1019. Research Institute, University of Dayton. July 1964.
9. Freudenthal, A. M. "Safety and the Probability of Structural Failure." Trans. A.S.C.E., Vol. 121 (1956), p. 1337.
10. Federal Aviation Agency. Civil Aeronautical Manual 4b. Washington: Superintendent of Documents, September 1962.

11. Civil Aeronautics Board. Resume of U. S. Civil Air Carrier and General Aviation Aircraft Accidents. Calendar years 1946-1960.
12. Williams, J. K. "Safety Factors," Journal of the Royal Aeronautical Society, Vol. 60, May 1956, p. 306.
13. Jost, G. S. and Patching, C. A. The Fatigue of 24-ST Aluminum Alloy Wings under Random Maneuver Loading. Aeronautical Research Laboratories (Australia) Report SM295. 1964.
14. Patching, C. A. "Fatigue in Aircraft Structures," The Journal of the Institution of Engineers (Australia), Vol. 34, September 1962, pp. 205-214.
15. Ford, D. G. Maximum Likelihood Estimators for Truncated Samples from Normal Distributions. Aeronautical Research Laboratories (Australia) S and M Report 264, October 1964.

Table 1
Service Load Data

$$\bar{F}_U(U) = \text{Pr} \{ \text{exceeding gust velocity } U(\text{f.p.s}) \}$$

$p_n(\Delta n)$ = probability density function for acceleration
increment $\Delta n(g)$

1. Atmospheric Gusts	
Type of Environment	Total gust counts (+ve and -ve)
(i) Thunderstorm (Fig. 1) $\bar{F}_U(U) = e^{-0.197U}$	14 per mile
(ii) Civil Airline Routes (Fig. 2) $\bar{F}_U(U) = 0.969e^{-0.344U} + 0.031e^{-0.208U}$	(see Fig. 3)
(iii) Lateral Gusts (Fig. 4) Low Level: $\bar{F}_U(U) = 0.000345e^{-0.143U}$ $+ 0.499655e^{-0.368U} + 0.41e^{-0.441U} + 0.09e^{-0.300U}$ High Level: $\bar{F}_U(U) = 0.032e^{-0.576U} + 0.968e^{-1.15U}$	2×10^3 per hour 720 per hour
2. Maneuver Accelerations	
Type of Operation	Total No. of Acceleration counts
(i) Fighter Aircraft (Fig. 5) $p_n(\Delta n) = \frac{2}{\sqrt{2\pi}\sigma_n} \cdot e^{-\frac{(\Delta n)^2}{2\sigma_n^2}}$ with: Ground attack A-A (Fig. 5) $\sigma_n = 1.97$ Ground attack C-C (Fig. 5) $\sigma_n = 1.65$ Interceptor F-F (Fig. 5) $\sigma_n = 1.70$ General mission $\sigma_n = 1.27$	35 per hour 40 per hour 43 per hour 10 per hour

(ii) Heavy Bomber (with equivalent vertical load factor Δn_z) (Fig.6)	N per hour
Δn_z upward: $\bar{F}(\Delta n_z) = 0.00314e^{-11.7 n_z} + 0.997e^{-23.6\Delta n_z}$	N per hour
Δn_z downward: $\bar{F}(\Delta n_z) = 0.00225e^{-14.39\Delta n_z} + 0.998e^{-28.78\Delta n_z}$	N per hour
with: $\Delta n_z = (n_z - 0.72)$, N = 6000 high altitude cruise	
$\Delta n_z = (0.68 - n_z)$, N = 6400 low level	

Table 2

Variation in Amount of Turbulence with Altitude⁶

Altitude, ft.	Percent flight distance in turbulence	
	Non-thunderstorm turbulence	Thunderstorm turbulence
0 to 10,000	18.0	0.10
10,000 to 20,000	6.4	0.11
20,000 to 30,000	4.5	0.062
30,000 to 40,000	3.9	0.0067
40,000 to 50,000	3.4	0.0017
50,000 to 60,000	2.2	0

Table 3. Data on Ultimate Strength of Structures

Group Symbol	Type of Specimen	Type of Loading	No. of Tests	Standard Deviation S	Significance Level	
					$\sigma_x = 0.05638$	$S_x = 0.04344$
STRUCTURES	A Typhoon Tailplane: Semi-Span	Bending	14	0.02930	* *	N.S.
	B Typhoon Tailplane Modified: Semi-Span	Bending	19	0.02200	* *	* *
	C Hudson Tailplane: Semi-Span	Bending	6	0.01740	* *	*
	D Whitley Tailplane: Semi-Span	Downward Bending	13	0.04610	N.S.	N.S.
	E Whitley Tailplane: Semi-Span	Upward Bending	7	0.03280	N.S.	N.S.
	F Whitley Tailplane: Semi-Span	Torsion	21	0.06010	N.S.	*
	G Mustang Wings: Asymmetric	Bending	5	0.04540	N.S.	N.S.
	H F-80 Tailplane	Bending	7	0.08180	N.S.	* *
	I F-86D Tailplane	Bending	3	0.09940	* *	* *
	J M.I.T. Results Speciman Type 1	Bending	3	0.04080	N.S.	N.S.
	K M.I.T. Results Speciman Type 2	Bending	3	0.01490	N.S.	N.S.
	Box-Beam Tests	Bending	9	0.03220	*	N.S.
COMPONENTS	L Convair: Wing Lower Surface Plate Stringer, J and L Type Stiffener	Compression	15	0.05570	N.S.	N.S.
	M Convair: Wing Lower Surface Plate Stringer, J Type Stiffener	Compression	7	0.07561	N.S.	* *
	N Convair: Wing Upper Surface Plate Stringer, Stringer Type "A"	Compression	12	0.01760	* *	* *
	O Convair: Wing Upper Surface Plate Stringer, Stringer Type "B"	Compression	6	0.03475	N.S.	N.S.
	P Convair: Wing Upper Surface Plate Stringer, Stringer Type "C"	Compression	6	0.01301	* *	* *
	Q Convair: Wing Upper Surface Plate Stringer, Stringer Type "D"	Compression	6	0.01625	* *	*
	R Douglas: Fuselage Frame Type "A"	Compression	4	0.01906	*	N.S.
	S Douglas: Fuselage Frame Type "B"	Compression	4	0.00971	* *	* *
		Total:	170			

Not Significant N.S.	10/20	10/20
Significant At 5%	2/20	3/20
Significant At 1%	8/20	7/20

Table 4

Reliability Calculations

(a) Gust Loads

$$P_F(x) = P_F \{ R < \mu_R (x+1) \} = \int_{-1.0 + \delta}^x p_x(x) \cdot \bar{F}_u(x) \cdot dx$$

$$\text{where } p_x(x) = \begin{cases} \frac{2 \sigma x^3}{\pi (\sigma x^2 + x^2)^2} & -0.2 \leq x < \infty \\ \frac{4.6955}{x+1} e^{-\frac{(\log [x+1])^2}{.00272}} & -1 \leq x \leq -0.2 \end{cases}$$

and $F(x)$ has the forms shown in the following cases:

Thunderstorm (1, (i)
Table I)

1. Uppgust Case

$$F_1(x) = e^{-\frac{0.197}{Kn} e^{-\frac{0.197 \sqrt{x+1}(1+66Kn)}{\alpha_{R,p} Kn}}}$$

$$\text{and } \delta = \frac{\alpha_{R,p}}{(1+66Kn)^{\sqrt{v}}}, \quad U_q = 66 \text{ f.p.s.}$$

$$(i) \bar{v}=1.5:Kn = .0227, .0303$$

$$\alpha_{R,p} = .\alpha_{47} \quad .0363, .0454$$

$$(ii) \bar{v}=1.5:Kn = .0227, .0303$$

$$\alpha_{R,p} = 1.0 \quad .0363, .0454$$

$P_F = P_F(x=\infty)$
shown in Fig. 14
for $F_1(x)$ and
 $F_2(x)$

Table 4 Continued

<p>2. Downgust Case</p>	$F_2(x) = e^{-\frac{0.197}{Kn} x} e^{-\frac{0.197}{\alpha_{R,p} Kn} (x+1)} (66Kn^{-1})$ <p>and $\delta = 0, U_q = 66$</p>	<p>(iii) $K_n = .0363: \bar{v} = 1.0, 1.25$ $\alpha_{R,p} = .947 \quad 1.50, 1.75$</p> <p>(iv) $K_n = .0363: \bar{v} = 1.0, 1.25$ $1.50, 1.75$ $\alpha_{R,p} = 1.0$</p>	<p>$P_F(x)$ shown in Figs. 10 and 11 for $F_1(x)$ and in Figs. 12 and 13 for $F_2(x)$. P_F for $F_1(x)$ and $F_2(x)$ combined in Fig. 15.</p>										
<p><u>General Gust Case</u> (1, (ii) Table 1)</p>	$F_3(x) = 0.969 e^{-50x} \times .344 \bar{v}(x+1) + 0.208 e^{-50x} \times .208 \bar{v}(x+1)$ <p>$U_q = 50, \delta = 0$</p>	<p>$\bar{v} = 1.0, 1.25, 1.50, 1.75$</p>	<table border="1"> <thead> <tr> <th>\bar{v}</th> <th>$P_F(x=0)$</th> </tr> </thead> <tbody> <tr> <td>1.0</td> <td>1.13×10^{-6}</td> </tr> <tr> <td>1.25</td> <td>8.89×10^{-8}</td> </tr> <tr> <td>1.50</td> <td>7.44×10^{-9}</td> </tr> <tr> <td>1.75</td> <td>6.53×10^{-10}</td> </tr> </tbody> </table>	\bar{v}	$P_F(x=0)$	1.0	1.13×10^{-6}	1.25	8.89×10^{-8}	1.50	7.44×10^{-9}	1.75	6.53×10^{-10}
\bar{v}	$P_F(x=0)$												
1.0	1.13×10^{-6}												
1.25	8.89×10^{-8}												
1.50	7.44×10^{-9}												
1.75	6.53×10^{-10}												
<p><u>Lateral Gust</u> (1, (iii) Table 1)</p> <p>1. Low Level</p> <p>2. High Level</p>	<p>$F_4(x) = 0.000345 e^{-.143 U_0(x+1)} + 0.499655 e^{-.368 U_0(x+1)}$</p> <p>$+ 0.41 e^{-.441 U_0(x+1)} + 0.09 e^{-.300 U_0(x+1)}$</p> <p>and $\delta = 0$</p> <p>$F_5(x) = 0.032 e^{-.576 U_0(x+1)} + 0.968 e^{-1.15 U_0(x+1)}$</p> <p>and $\delta = 0$</p>	<p>$U_0 = 89 \text{ f.p.s.}$</p> <p>$U_0 = 89 \text{ f.p.s.}$</p>	<p>$P_F = 1.29 \times 10^9$</p> <p>$P_F = 1.53 \times 10^{20}$</p>										

Table 4 Continued

<u>Vertical Acceleration</u> (Heavy Bomber 2,(ii) Table I)			
1. Upward	$F_6(x) = 0.00314e^{-11.7[3(x+1)-N_0]} + 0.997e^{-23.6[3(x+1)-N_0]}$ <p>and $\delta = \frac{N_0}{3}$</p>	$N_0 = 0.72$ $N_0 = 0.68$	$P_F = 1.60 \times 10^{-13}$ $P_F = 1.00 \times 10^{-13}$
2. Downward	$F_7(x) = 0.00225e^{-14.39[(x+1)+N_0]} + 0.998e^{-28.78[(x+1)+N_0]}$ <p>and $\delta = 0$</p>	$N_0 = 0.72$ $N_0 = 0.68$	$P_F = 5.46 \times 10^{-14}$ $P_F = 9.71 \times 10^{-14}$

(b) Manoeuvre Loads

$$P_F(y) = P_F \{S < \mu_R (y+1)\} = \int_{-1+\delta}^y b_n(y) \cdot P_x(y) \cdot dy - P_x(\delta-1) \int_{\delta-1}^y b_n(y) \cdot dy$$

$$\text{where } P_x(y) = \begin{cases} \frac{0.6096}{11.3} (y+1)^{11.3} & : -1 \leq y \leq -0.2 \\ \frac{\sigma_x y}{\pi(\sigma_x^2 + y^2)} + \frac{1}{\pi} \arctan \frac{y}{\sigma_x} + 1/2 & : -0.2 \leq y < \infty \end{cases}$$

$$P_F(x) = P_F(y) + [1 - P_n(y)][P_x(y) - P_x(\delta-1)]$$

Table 4 Continued

Calculate $P_F(y)$ and hence $P_F(x)$ for the following cases.

<p>1. <u>Manoeuvre Loads</u></p>	$p_n(y) = \frac{2N_u}{\sqrt{2\pi}\delta_n} e^{-\frac{[(y+1)Nu - 1]^2}{2\sigma_n^2}}$ <p>where $n_u = \bar{v}n_q$ and $\sigma = \frac{1}{n_u}$</p>	<p>(i) $N_q = 7 \frac{1}{3}$, $\bar{v} = 1.5$, $\alpha_A, \alpha = 1.0$ $\sigma_n = 1.27, 1.38, 1.65, 1.93$ 2.20</p> <p>(ii) $n_q = 8 \frac{2}{3}$, $\bar{v} = 1.5$, $\alpha_{R,p} = 1.0$ $\sigma_n = 1.69, 2.05$</p> <p>(iii) $n_q = 7 \frac{1}{3}$, and $\sigma_n = \frac{1.35}{\bar{v}}$ $\alpha_{R,p} = 1$, $\alpha_{R,p} = 0.947$ $\bar{v} = 1.0, 1.25, 1.50, 1.75$</p> <p>(iv) $n_q = 8 \frac{2}{3}$ and $\sigma_n = \frac{1.65}{\bar{v}}$ $\alpha_{R,p} = 1$, $\alpha_{R,p} = 0.947$ $\bar{v} = 1.0, 1.25, 1.50, 1.75$</p> <p>(v) $n_u = 9.2$ $\sigma_n = 1.98$</p>	<p>$P_F(x=\infty) - P_F(x=-0.25)$ shown as a function of σ_n in Fig. 17.</p> <p>$P_F(x=\infty) - P_F(x=-0.25)$ shown as a function of σ_n in Fig. 15.</p> <p>$P_F(x)$ and $P_F(y)$ shown in Fig. 16</p> <p>$P_F(x=\infty) - P_F(x=-0.25)$ $= 6.22 \times 10^5$</p>
----------------------------------	---	---	--

Table 4 Continued

<u>Thunderstorm</u>	$p_n(y) = p_u(y) = 66 \times 0.197 \bar{v}^{-66 \times 0.197 \bar{v}(y+1)}$ and $\delta = 0$	$\bar{v} = 1.5.$	$P_F(x)$ and $P_F(y)$ shown in Fig. 16.
---------------------	--	------------------	--

Table 5

Comparison of Failure Rates

(a) Ultimate Failure

Case	Service Data			Predicted Data	
	Hours	No. of Failures	Failure rate (per hour)	Case	Failure rate (per hour)
U.S. Civil Air Carrier	50×10^6	14	2.8×10^{-7}	Thunderstorm (Uppgust + Downgust $K_n = .0363$)	$1.6 \times 10^{-7} *$
U.K. Civil Aircraft	16×10^6	6	3.75×10^{-7}	General Gust Case (3 in Table 4a)	$1.5 \times 10^{-7} *$
Total for Civil Aircraft	66×10^6	20	3×10^{-7}		
Heavy Bomber					
(i) High Level - Tail Assembly	9.5×10^5	3 **	3×10^{-6}	Lateral Gust (Table 4 and Table 1)	1.1×10^{-17}
Mainplane	1.86×10^6	0		Uppgust and Downgust (From Table 4(a) and Table 1,2,(if))	1.3×10^{-9}
(ii) Low Level - Tail Assembly	1.5×10^5	3 **	2×10^{-5}	Lateral Gust (Table 4 and Table 1)	2.6×10^{-6}
Mainplane	1.28×10^5	0		Uppgust and Downgust (Table 4 and Table 1)	1.26×10^{-9}

(iii) Total for Mainplane 2×10^6		0	$< 5 \times 10^{-7}$	Combined (i and ii)	2.6×10^{-9}
Fighter	1.06×10^5	3	2.85×10^{-5}	Maneuver (Table 1 and Table 4) $n_u=9.2, \sigma_n=1.97$ $n_u=11$	$3 \times 10^{-4+}$ $6 \times 10^{-5+}$

**Refers to particular type of bomber.

*Calculated for cruising speed = 200 mph, height = 20,000 ft.

+Based on measured load counts in service = 5 counts per hour with $\sigma_n = 1.97$.

(b) Fatigue Failure

	Hours	No. of Failures	Failure rate (per hour)	Mean Estimated Life
U.S. Civil Air Carrier	50×10^6	6	2.4×10^{-7}	
U.K. Civil Aircraft	16×10^6	7	8.8×10^{-7}	
Total for Civil Aircraft	66×10^6	13	4×10^{-7}	
Heavy Bomber (final failure)	2×10^6	1	10^{-6}	5000 hours (approx.)
(initial failure)	2×10^6	19		1970 hours
Fighter (final failure)	1.06×10^5	nonde- tected		3100 hours
(initial failure)	1.06×10^5	10		480 hours

Table 6 - Fatigue Lives
Initial Failure of Heavy Bomber

N_i Average of N for interval i	Life in Hours (N)	M_{ti}	$\sum \frac{1}{M_{ti}}$	$P(N_i) = 1 - e^{-\sum \frac{1}{M_{ti}}}$
1407	1288	40	.0263	.026
	1434	39		
	1500 D	38		
	1504	37		
	1529	36		
	1538	35		
1589	1611	34	.0575	.056
	1708	33		
	1733 D	32		
	1743	31		
1743	1745	30	.0919	.088
	1753 D	29		
1756 1768 1784 1812	1754	28	.2489	.220
	1762 D	27		
	1774 D	26		
	1795 D	25		
	1830 D	24		
	1836	23		
	1841	22		
	1840	21		
	1856	20		
	1864	19		
1877	1877	18	.4579	.367
	1884 D	17		
	1898	16		
1894	1902 D	15	.5245	.408
	1904	14		
1924	1906 D	14	.5959	.449
	1917	13		
	1949 D	12		
1984 2019 2030	1994	11	.6792	.493
	2010 D	10		
	2028 D	9		
	2031 D	8		
2052 2081 2107	2052	7	1.0153	.637
	2075 D	6		
	2087 D	5		
	2128 D	4		
	2135	3		
2140	2158 D	2	2.1319	.881
	2190	1		

D = Defect

Table 7 Estimation of Fatigue Sensitivity Factors

(a) Fatigue sensitivity factor at seven life times

	Life to Initial Failure		Life to Final Failure	
	$N^* = \frac{\mu_n}{3}$	$W^* = \frac{1}{2}\mu_n$	$N^* = 1/3 \mu_n$	$W^* = \frac{1}{2}\mu_n$
(i) Bomber				
μ_n	1970 hrs.	1970 hrs.	5000 hrs.	5000 hrs.
$r_F \mu_n$ (from Fig.20)	1.58×10^{-9}	7×10^{-4}	1.58×10^{-9}	7×10^{-4}
r_F	8×10^{-13}	3.35×10^{-7}	3.16×10^{-13}	1.4×10^{-7}
r_u (complete airframe) from Table 5	2×10^{-7}	2×10^{-7}	2×10^{-7}	2×10^{-7}
$f(N^*) = \frac{r_F}{r_u}$	4×10^{-5}	1.8	1.6×10^{-6}	7×10^{-1}
$N^* = P_U(N)$	660 hrs.	985 hrs.	1670 hrs.	2500 hrs.
(ii) Fighter				
μ_n			3100	3100
$r_F \mu_n$ (from Fig.20)			1.58×10^{-9}	7×10^{-4}
r_F			5.1×10^{-13}	2.25×10^{-7}
r_u (from Table 5)			2.85×10^{-5}	2.85×10^{-5}
$f(N^*) = \frac{r_F}{r_u}$			1.8×10^{-8}	7.9×10^{-3}
$N^* =$			1030 hrs.	1550 hrs.

(b) Life time for equal failure risks

	Fighter	Bomber (initial failure)
μ_n	3100	1970
r_u	2.85×10^{-5}	2×10^{-7}
$\mu_n r_u(N_o) = \mu_n r_u$	8.83×10^{-2}	3.9×10^{-4}
$\frac{N_o}{\mu_n}$ (From Fig. 20)	.49	.61
$N_o = \left(\frac{N_o}{\mu_n}\right) \mu_n$	1900 hrs.	960 hrs.
$P_u(N_o) =$	5.6×10^{-2}	2×10^{-4}

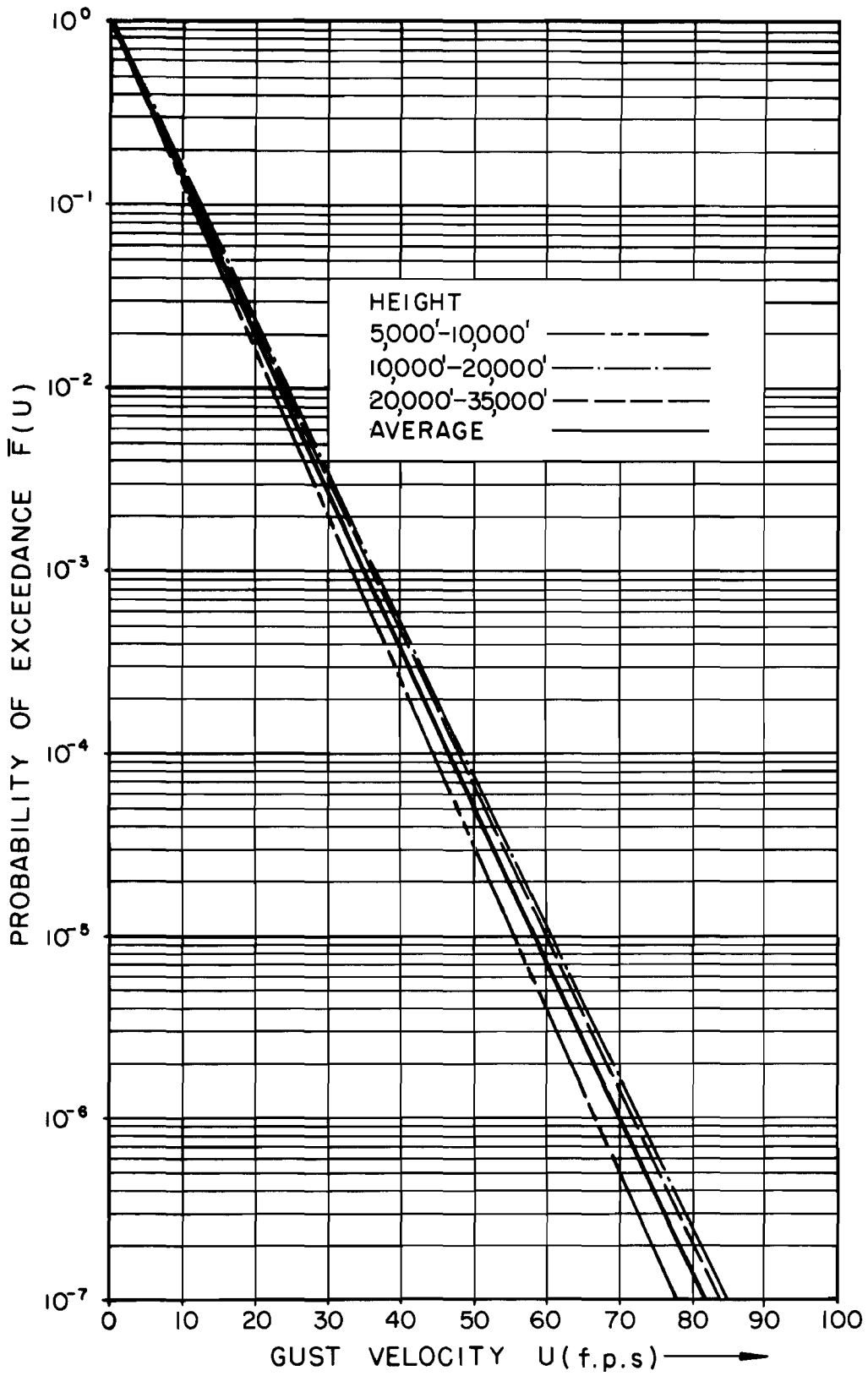


Fig. 1. Probability Distribution for Thunderstorm Gusts.

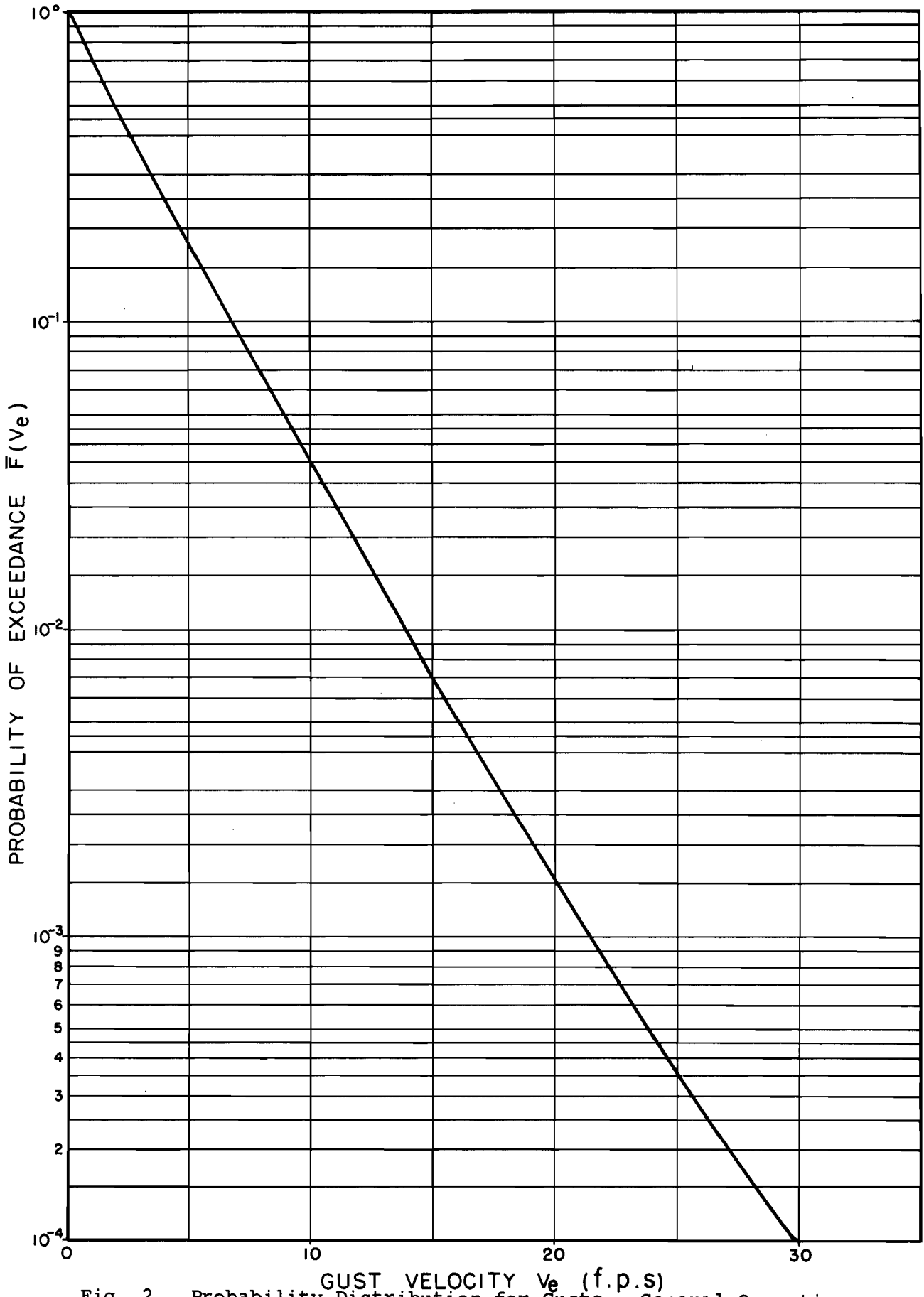


Fig. 2. Probability Distribution for Gusts. General Operation

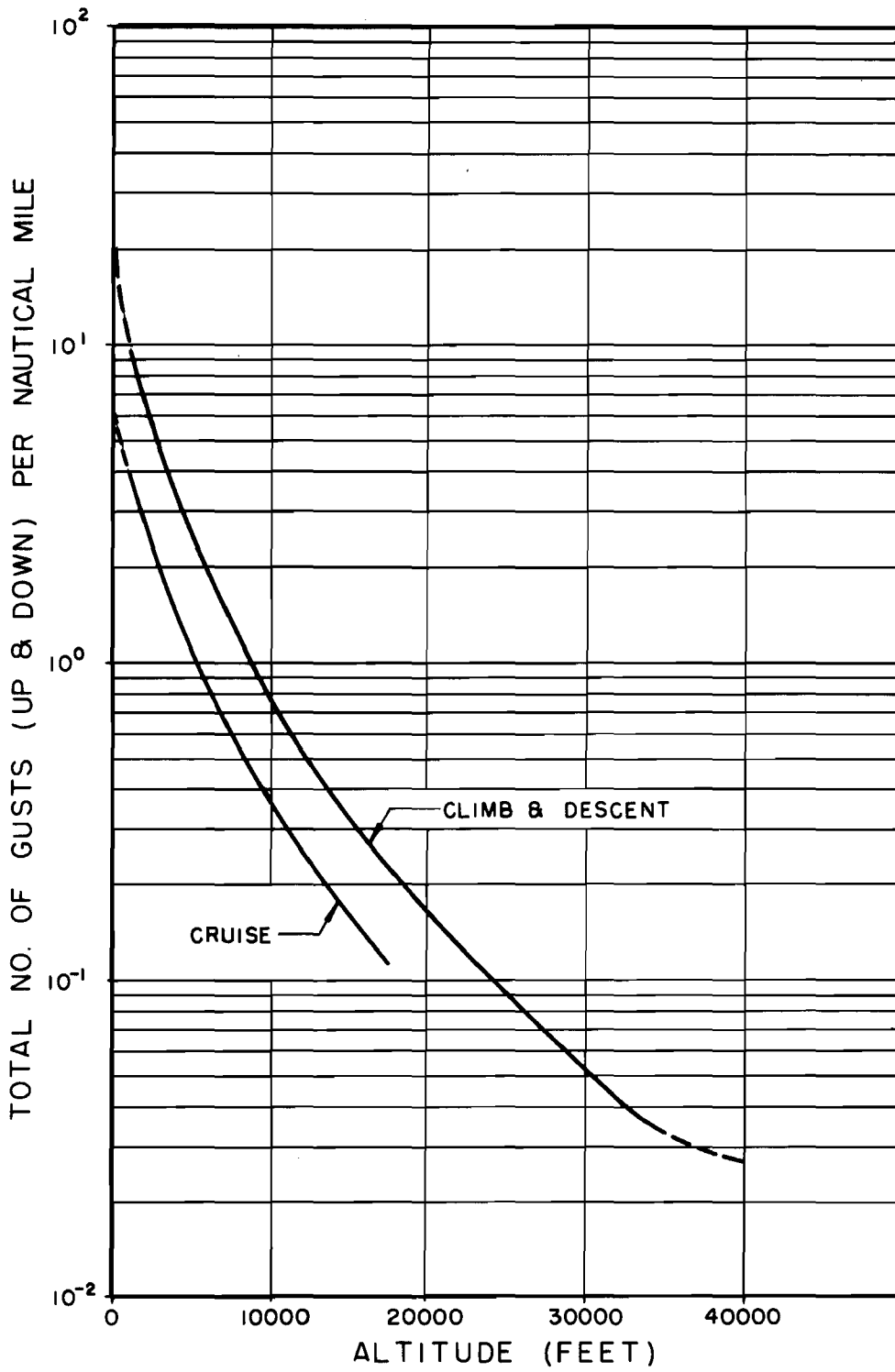


Fig. 3. Total Gust Counts per Mile. General Operation

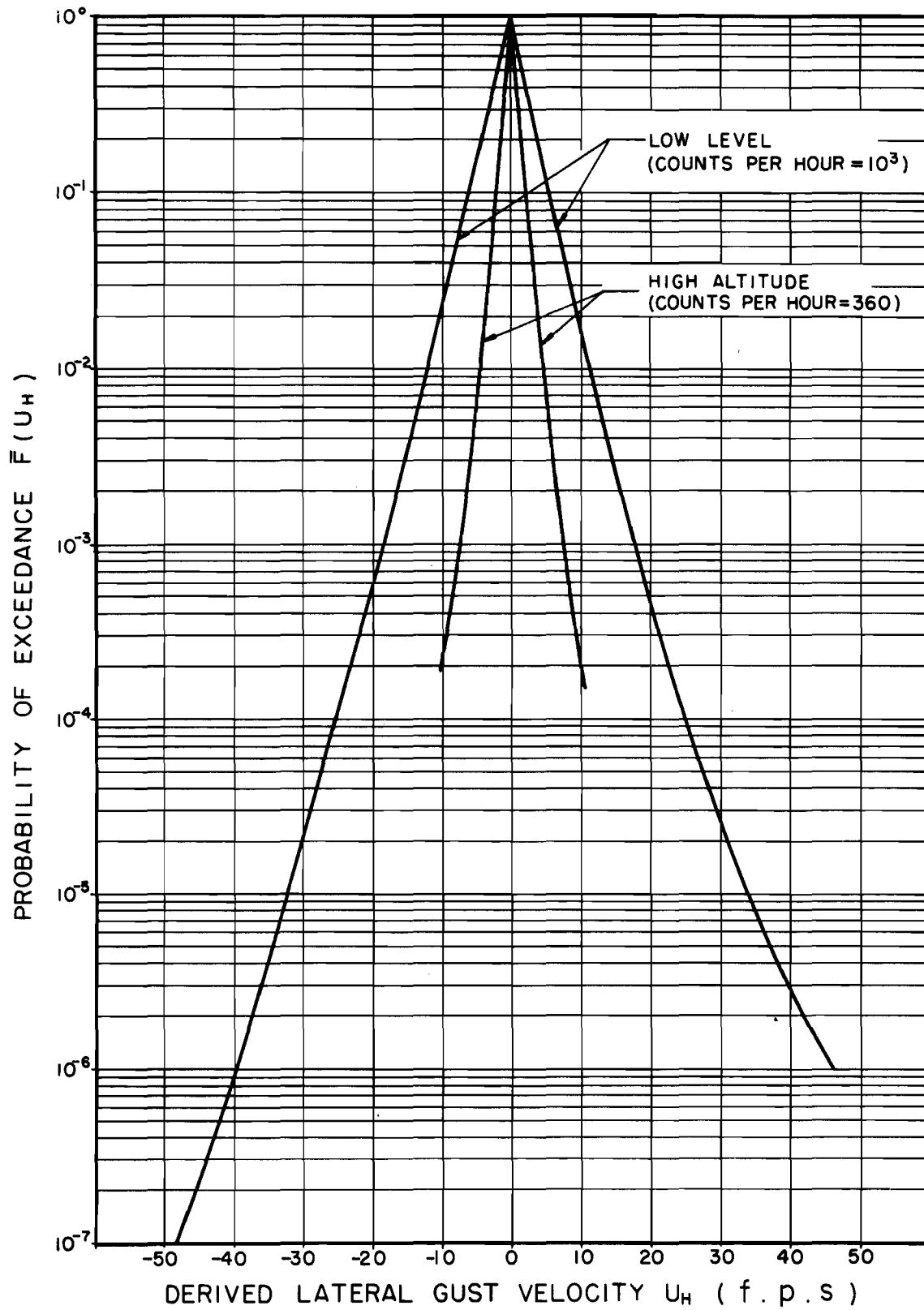


Fig. 4. Probability Distribution for Lateral Gusts.

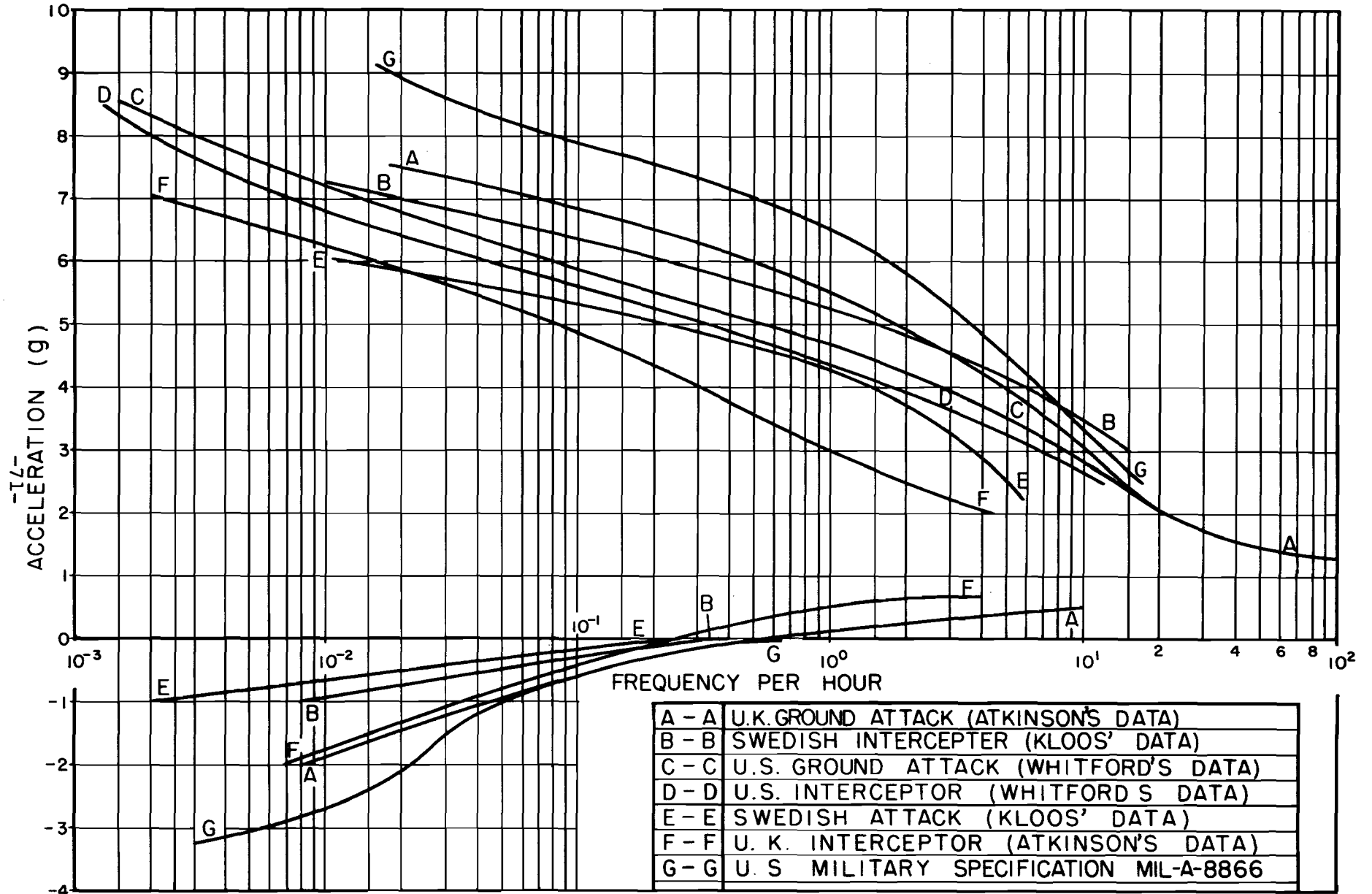


Fig. 5. Frequency Distributions for Maneuver Accelerations. Fighter Aircraft.

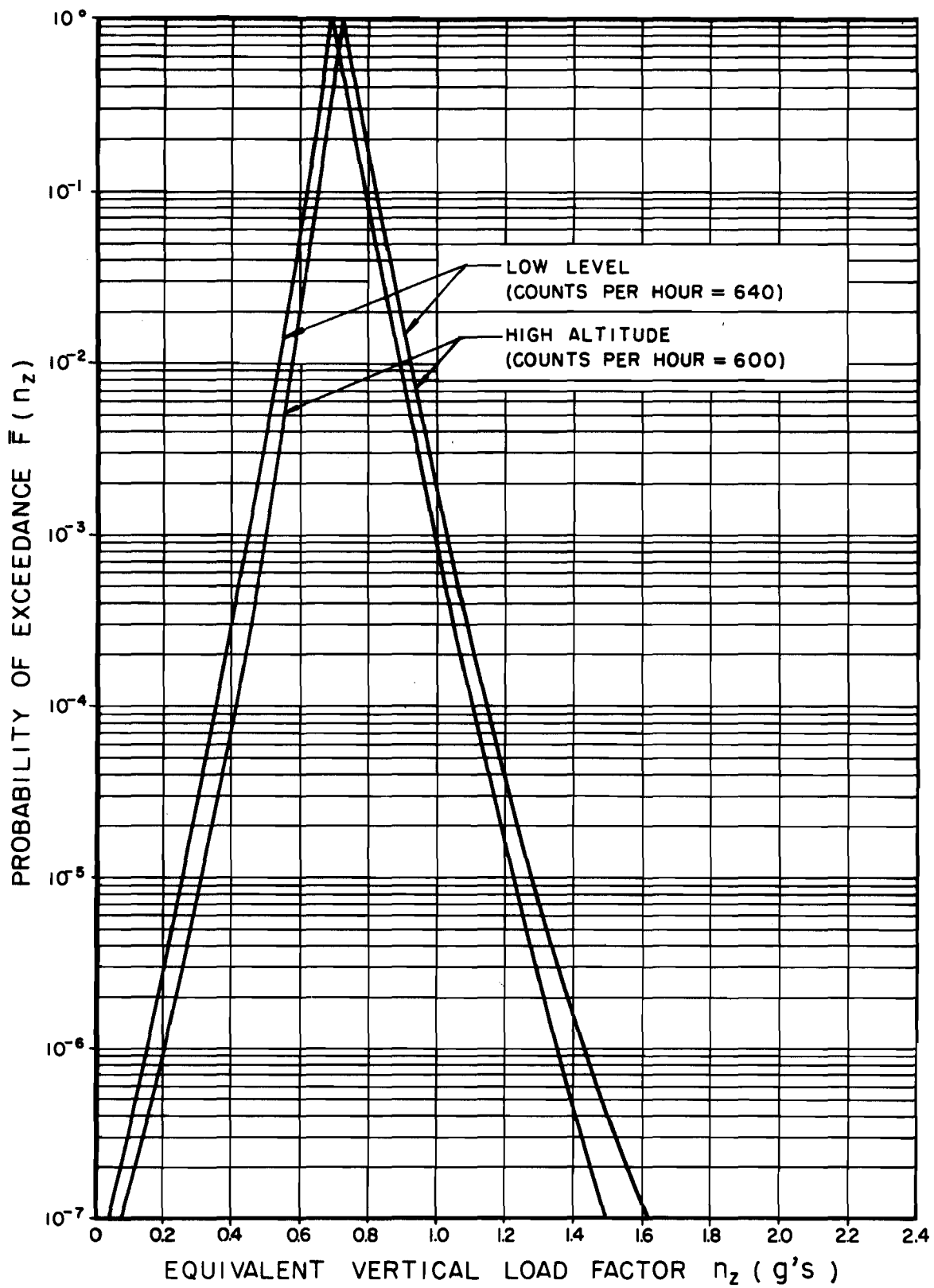
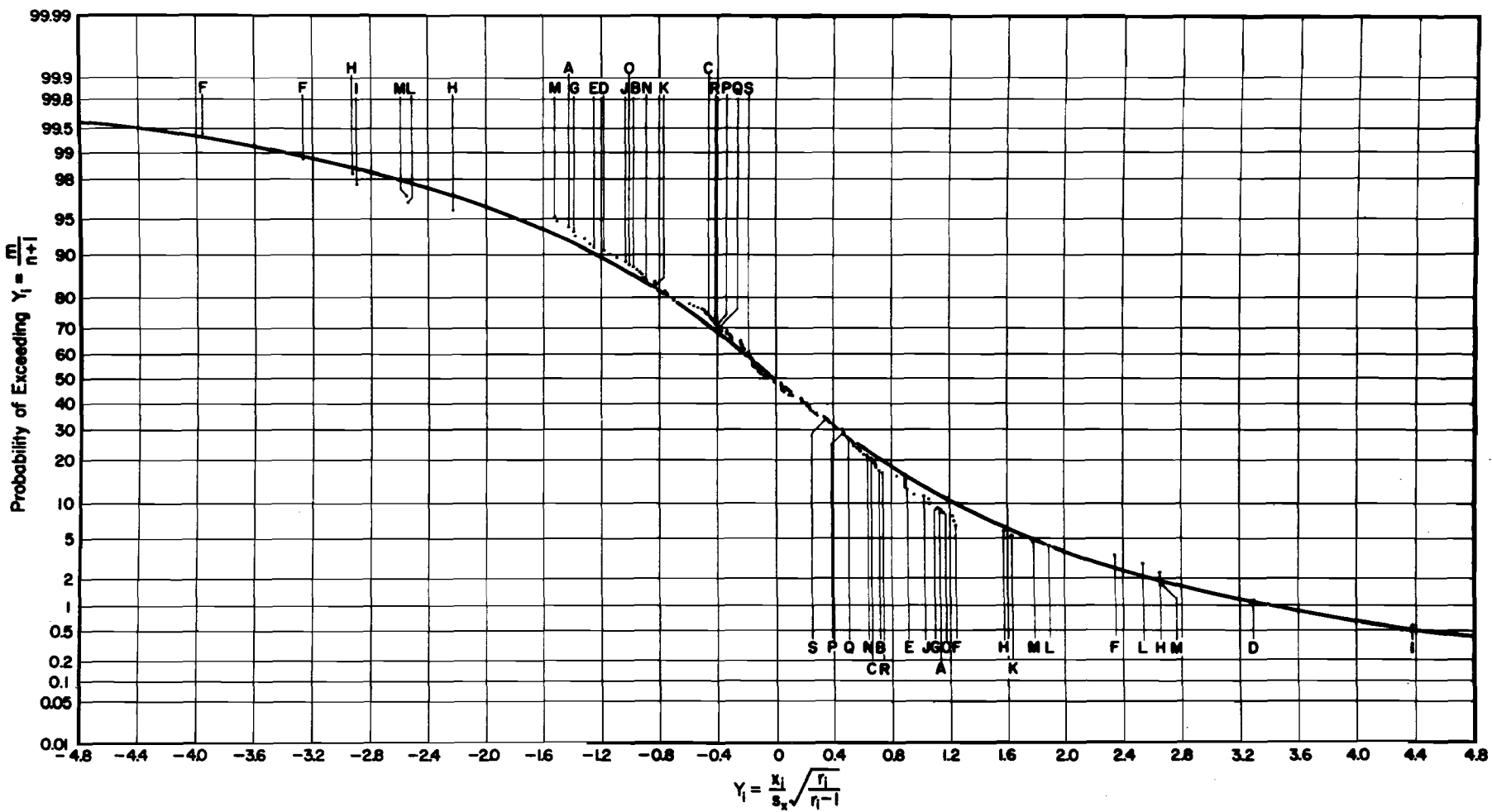


Fig. 6. Vertical Acceleration Data for Heavy Bomber.

Fig. 7. Probability Distribution for Structural Resistance



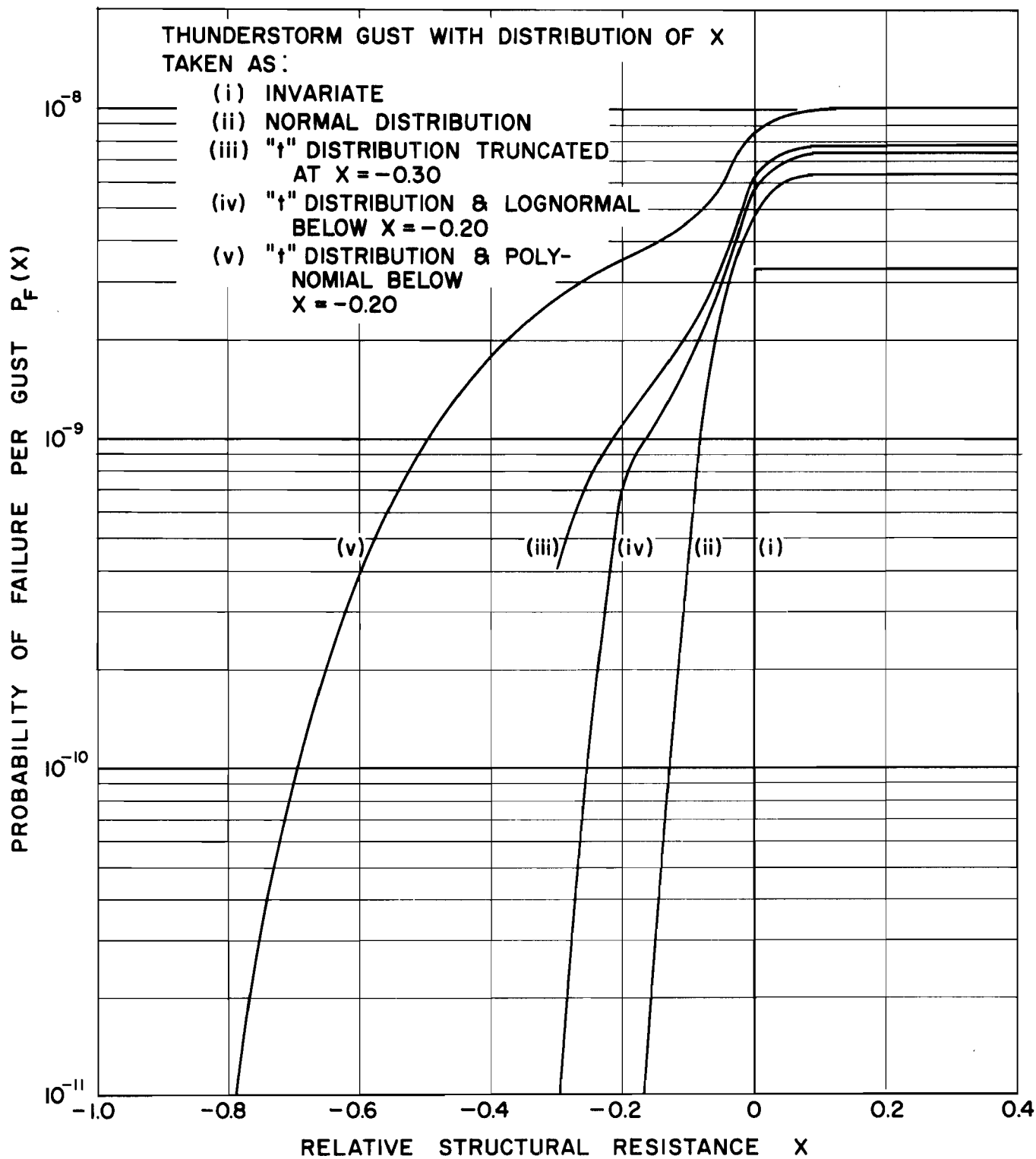


Fig. 9. Probability of Failure in Thunderstorm Gusts.

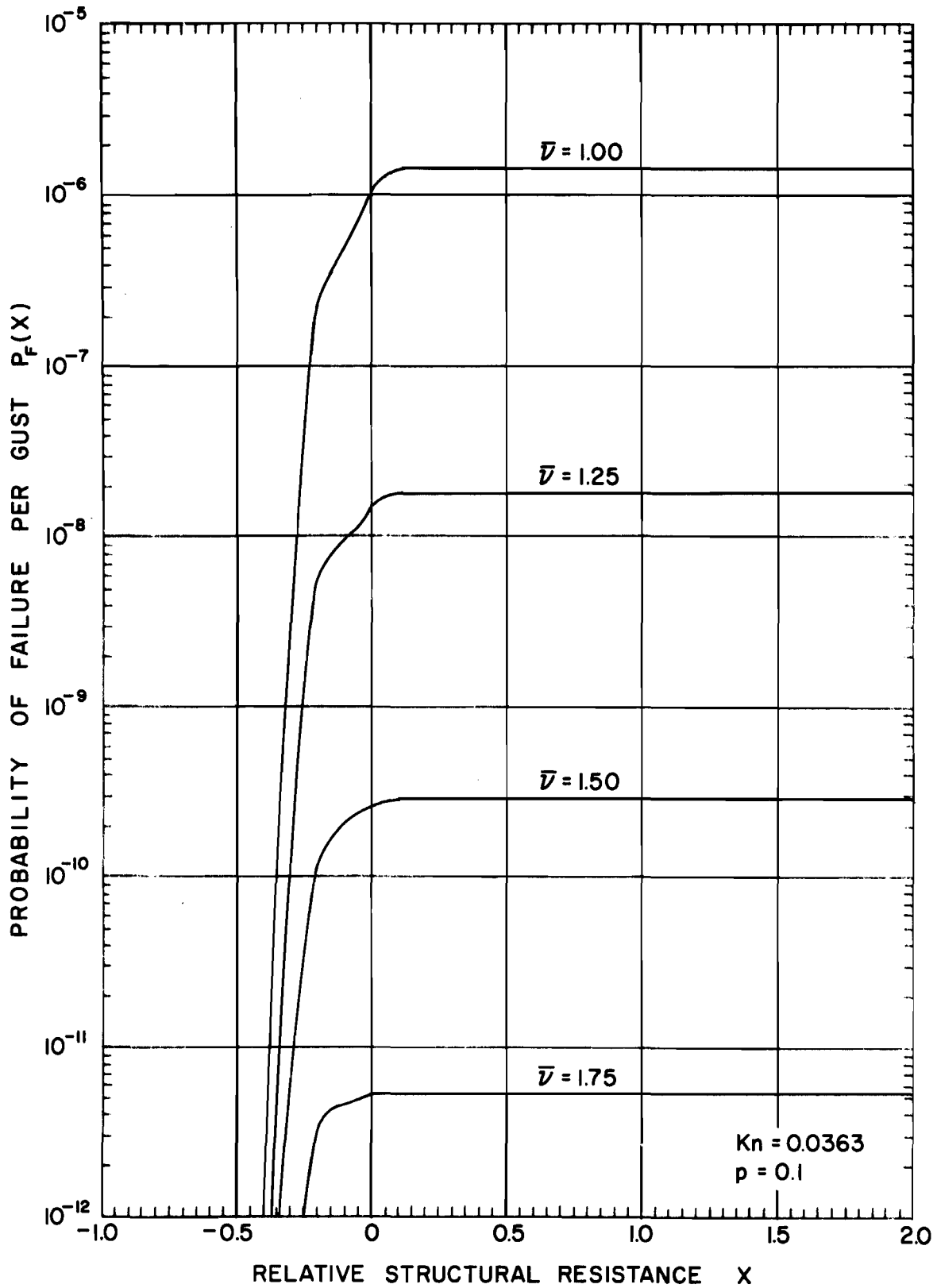


Fig. 10. Probability of Failure under a Thunderstorm Gust for Various Safety Factors: Upgust, $p = 0.1$.

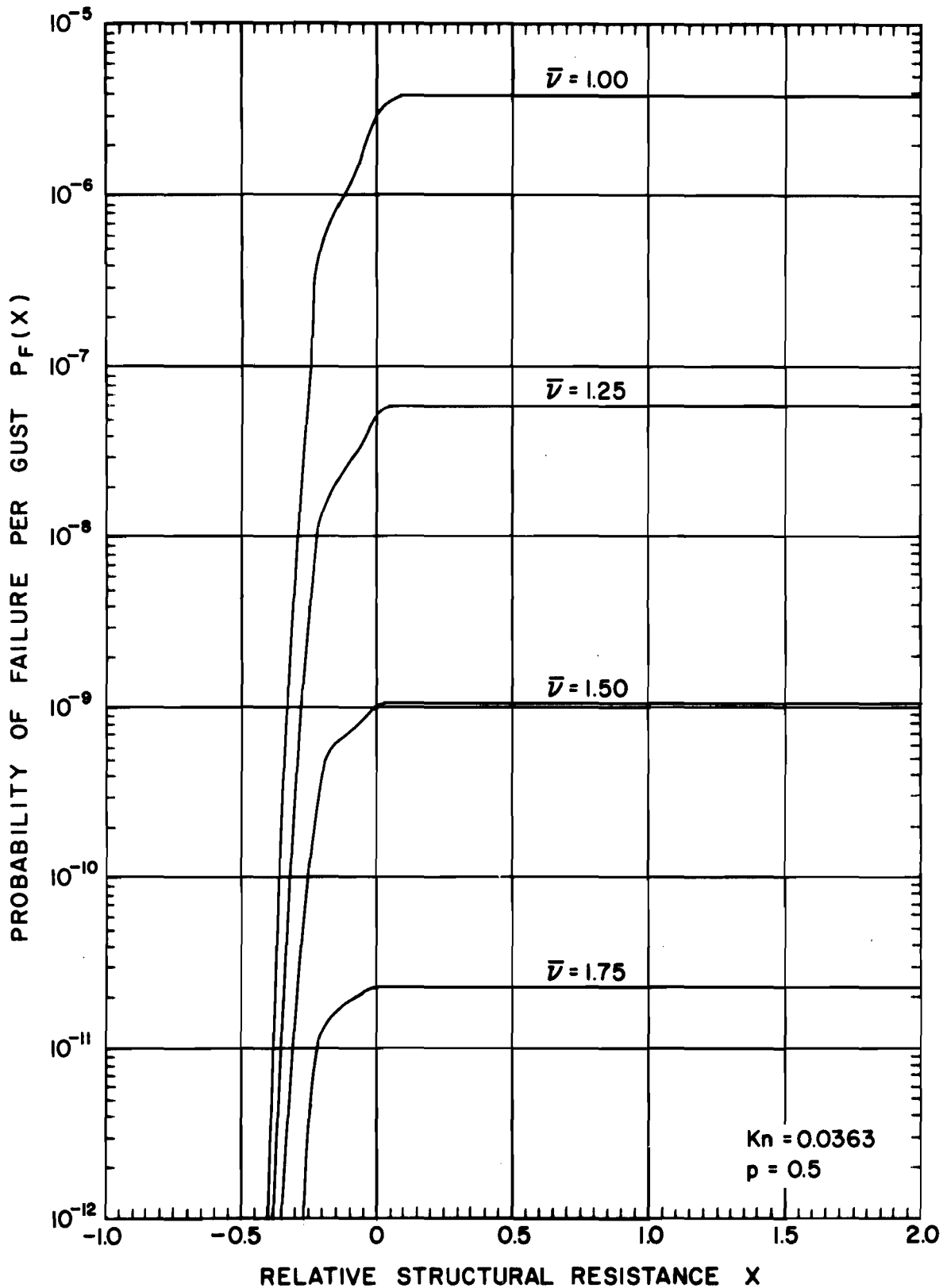


Fig. 11. Probability of Failure under a Thunderstorm Gust for Various Safety Factors: $U_{pgust}, p = 0.5$.

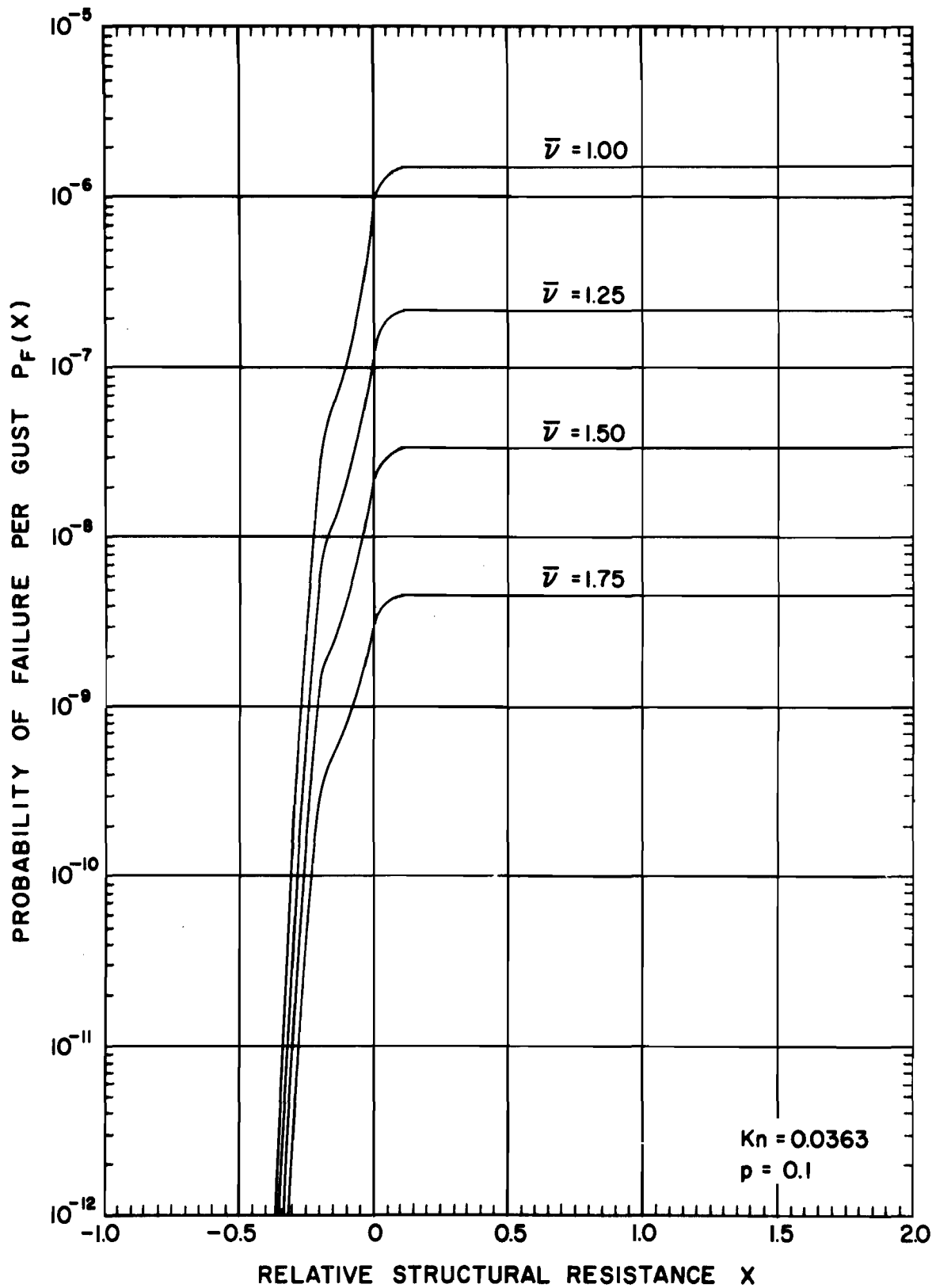


Fig. 12. Probability of Failure under a Thunderstorm Gust for Various Safety Factors: Downgust, $p = 0.1$.

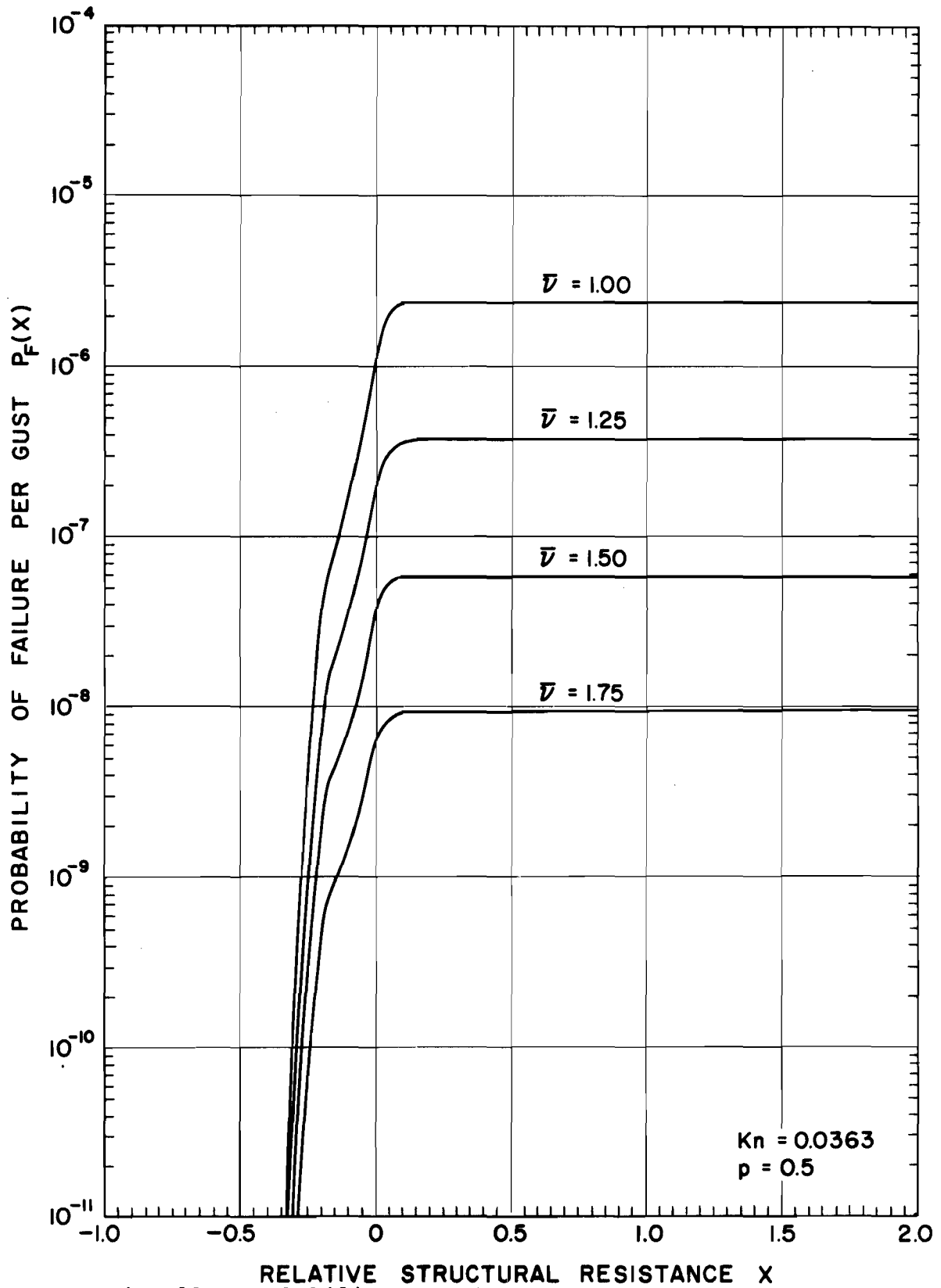


Fig. 13. Probability of Failure under a Thunderstorm Gust
 for Various Safety Factors: Downgust, $p = 0.5$

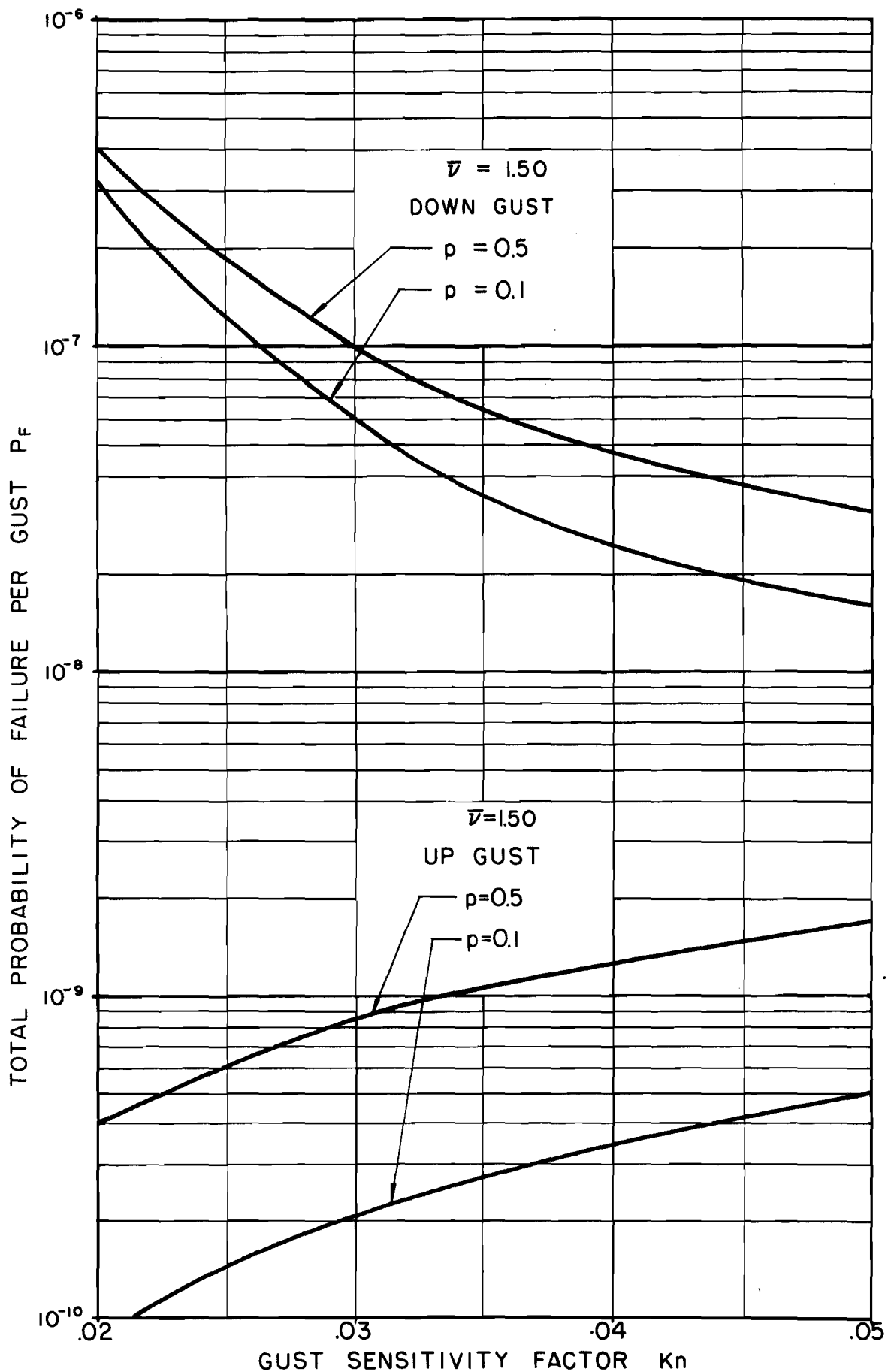


Fig. 14. Probability of Failure under a Thunderstorm Gust as a Function of K_n .

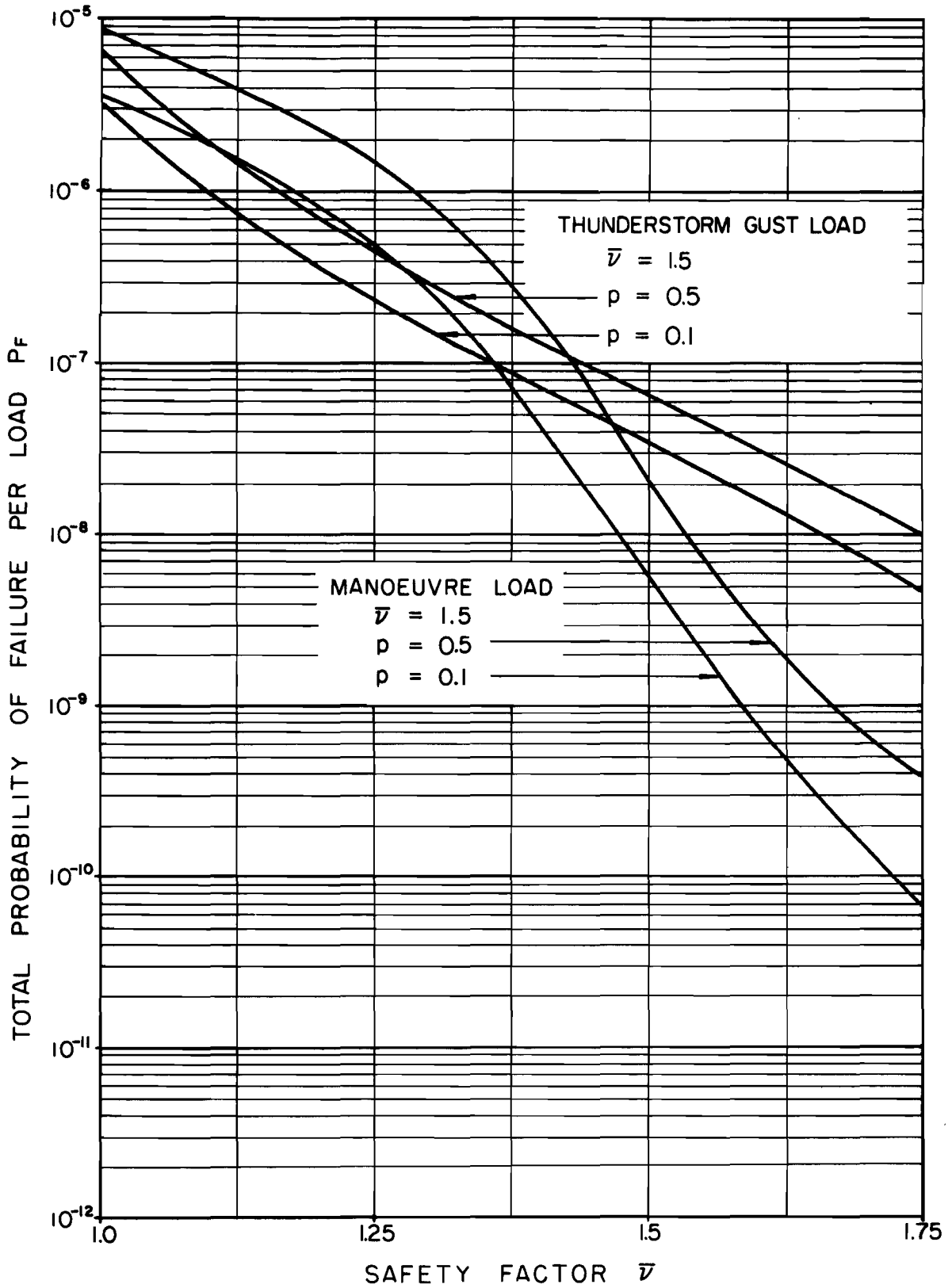


Fig. 15. Probabilities of Failure as a Function of v .

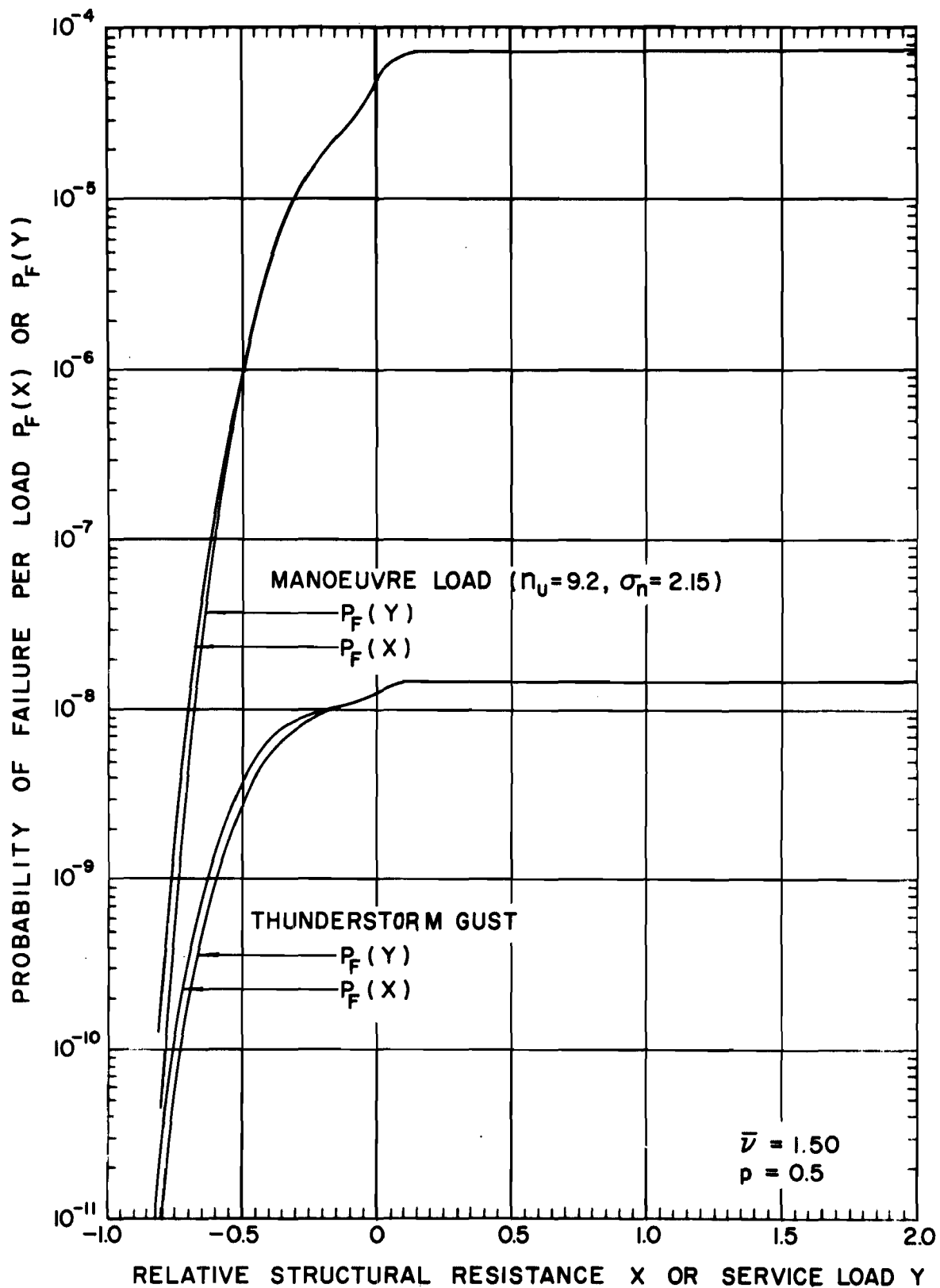


Fig. 16. Probability of Failure as a Function of Structural Resistance R and Service Load S.

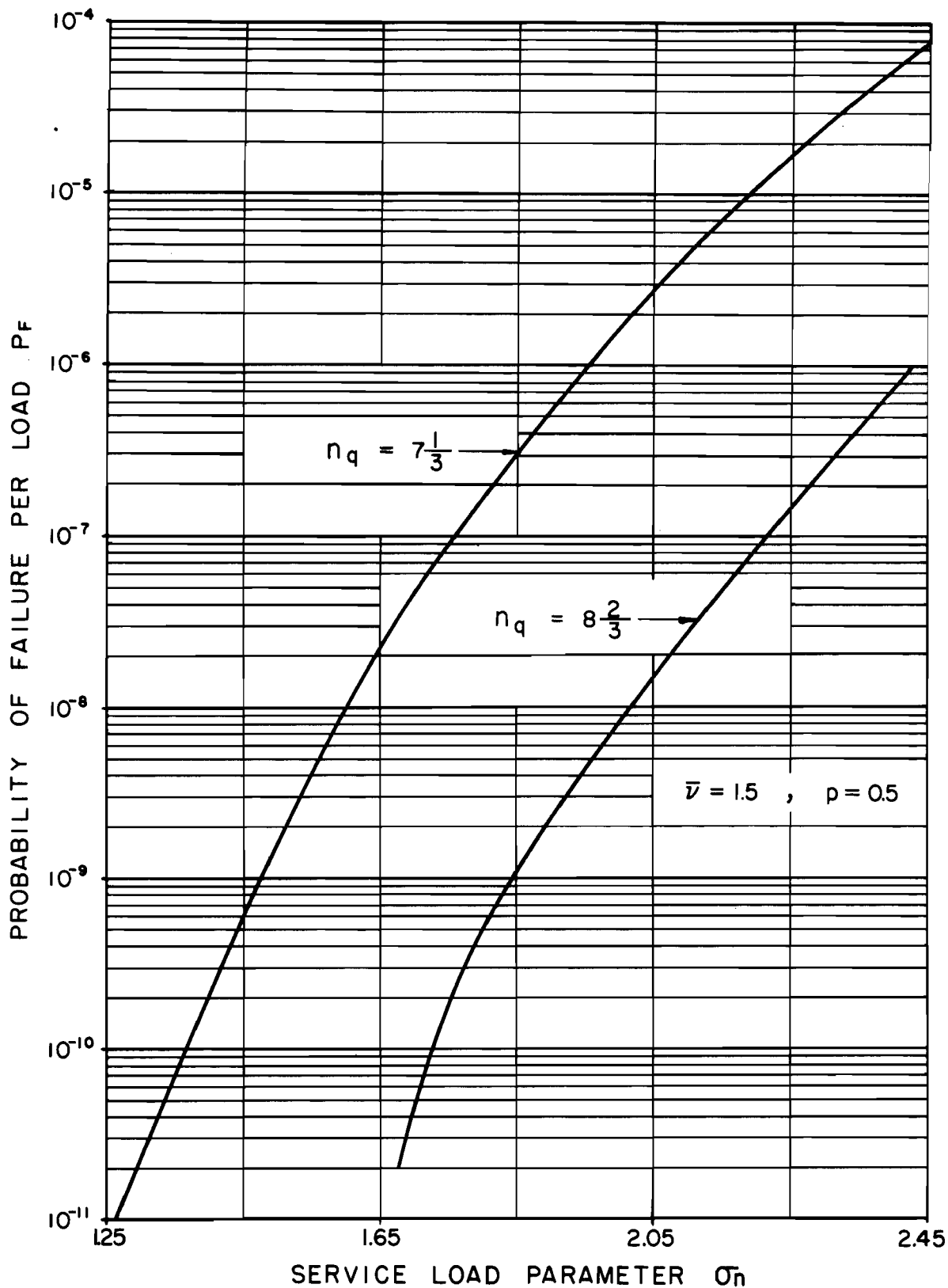


Fig. 17. Probability of Failure of Fighter Aircraft in Various Missions.

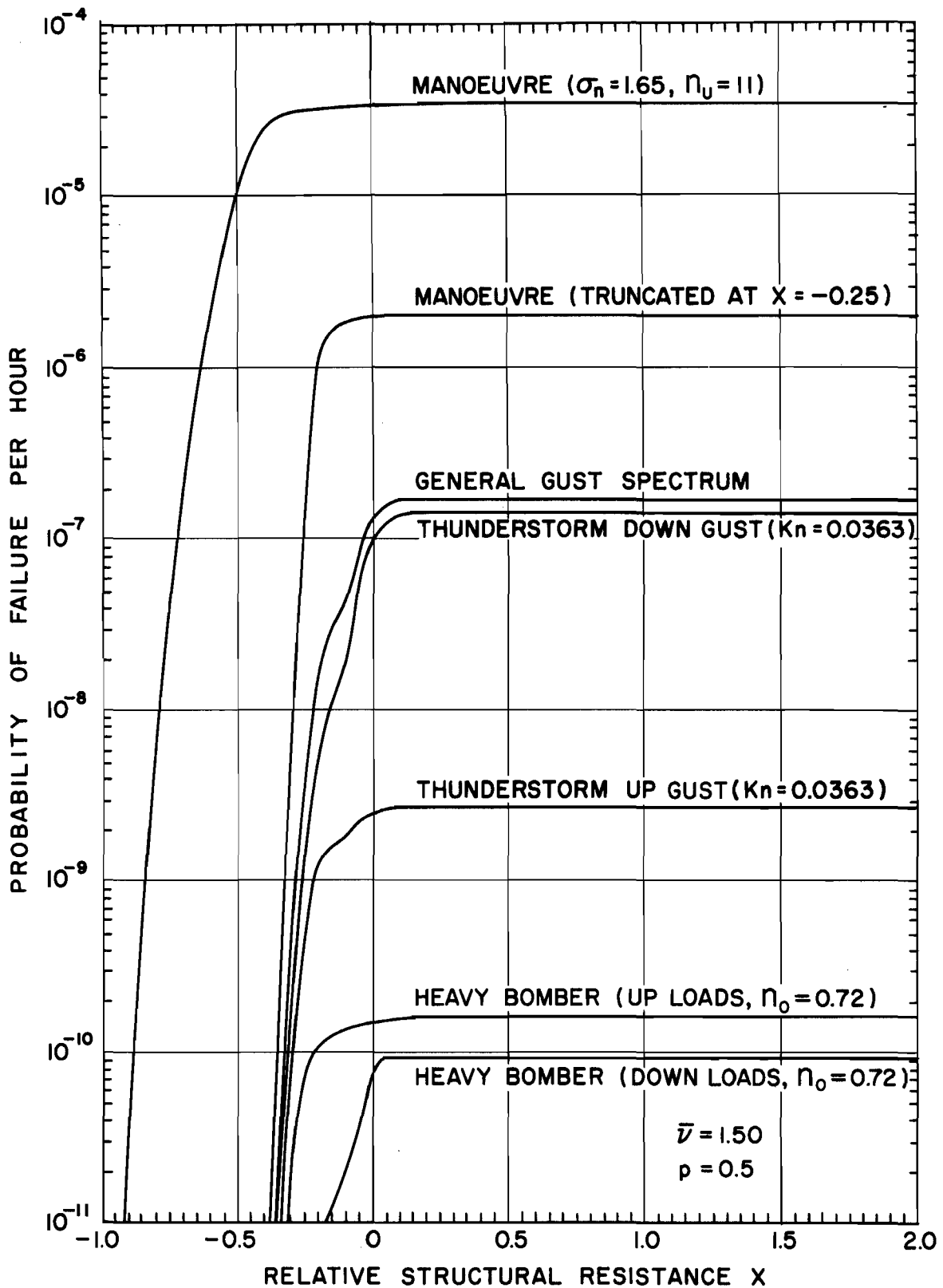


Fig. 18. Comparison of Failure Rates under Various Load Spectra.

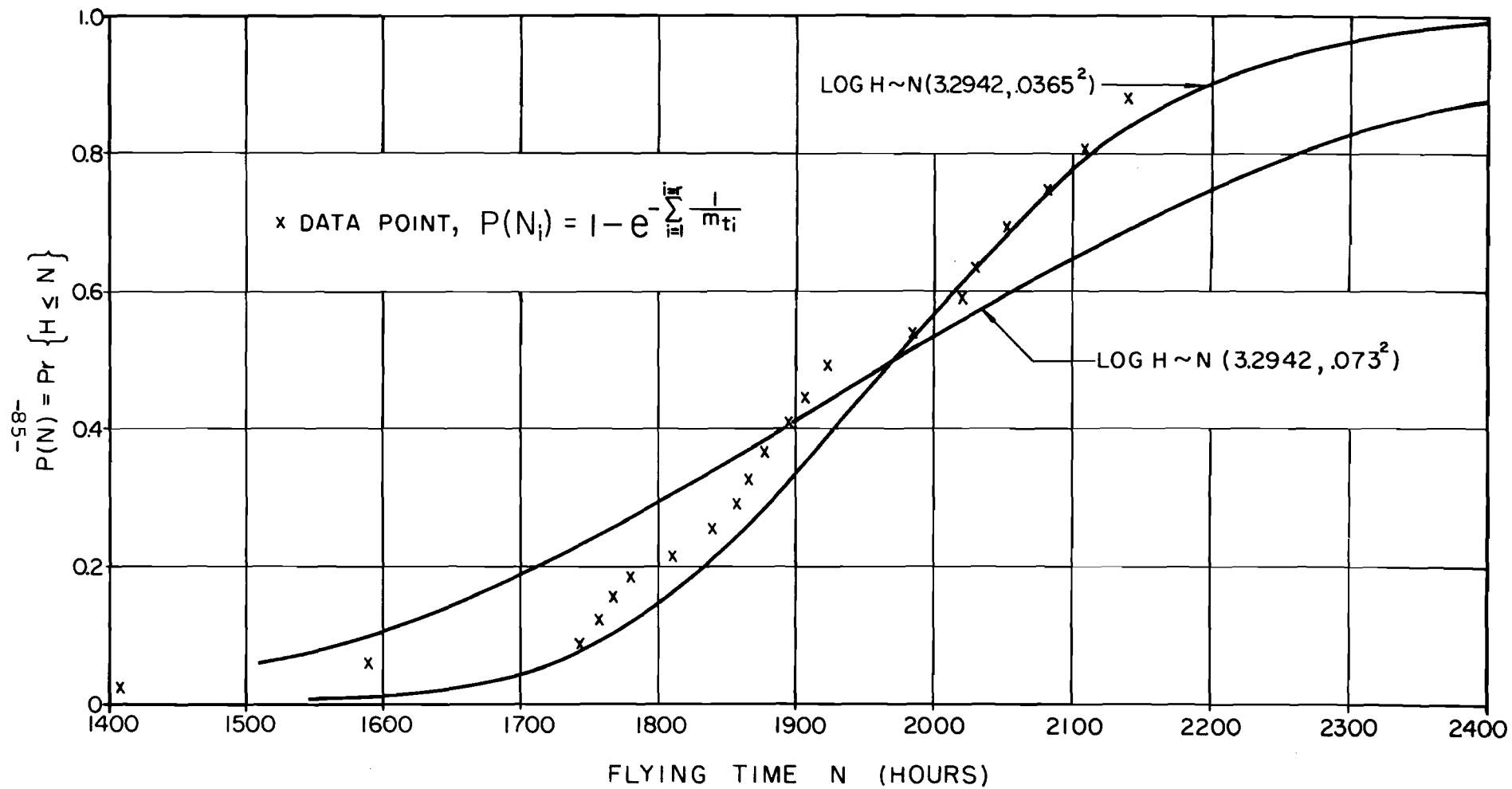


Fig. 19. Probability Distribution of Fatigue Life for Heavy Bomber.

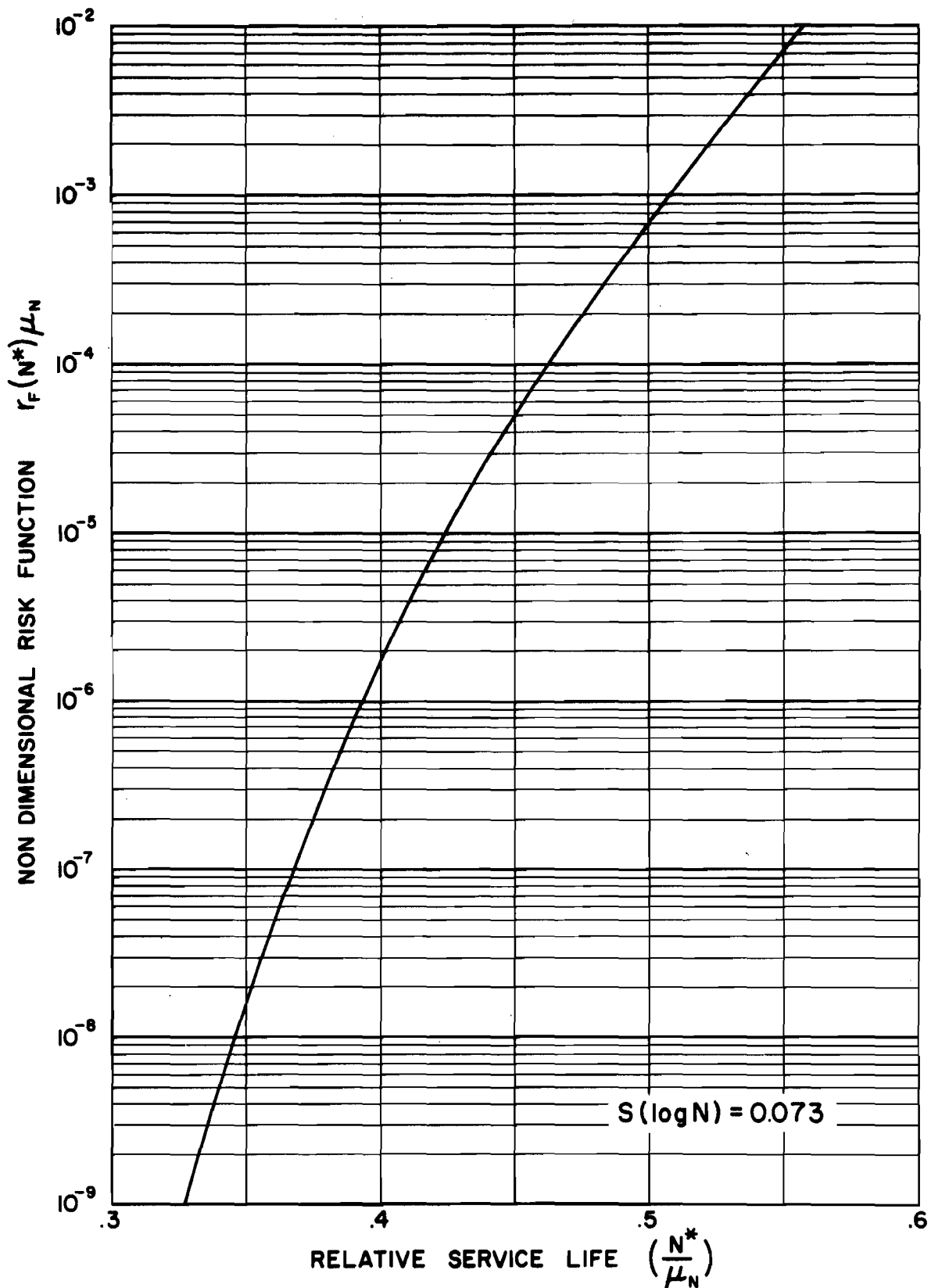


Fig. 20. Non-Dimensional Risk Function (Log Normal Distribution).